EFFECT OF FIBER TYPE ON MECHANICAL PROPERTIES AND DURABILITY ASPECTS OF FIBER REINFORCED CONCRETE

by

Alexandros Dimoutsis

B.Sc., Civil Engineering, University of Edinburgh, 2005

Submitted to the Institute for Graduate Studies in
Science and Engineering in partial fulfillment of
the requirements for the degree of
Master of Science

Graduate Program in Civil Engineering

Boğaziçi University

2009

ACKNOWLEDGMENTS

I would like to express my gratitude to all the people who in one way or another contributed to the development of this research. I would like to express my sincere appreciation to my advisor Prof. Dr. Turan Özturan and my co-advisor Assist. Prof. Dr. Altuğ Söylev; thank you for your valuable help in instructing, guiding and supporting me throughout the duration of this project.

Also, I would like to thank the members of my Master's thesis examination committee: Assoc. Prof. Dr. Cem Yalçın, Assist. Prof. Dr. Nilüfer Özyurt and Prof. Dr. Hulusi Özkul for their knowledgeable and in-depth comments and advice.

Special thanks to Ümit Melep for his technical assistance and labor, without which the experimental testing of this research would not be possible, and for making my lab days more enjoyable.

Further, I would like to thank my friends and colleagues: C. Aydın, D. Uluğtekin, İ. Şanal, M. Ülker and U. Karacadağlı for their help, the support and for the fun times during our MSc. I wish you all success, luck and happiness.

Finally, I would like to thank my family for their continuous support and encouragement.

ABSTRACT

EFFECT OF FIBER TYPE ON MECHANICAL PROPERTIES AND DURABILITY ASPECTS OF FIBER REINFORCED CONCRETE

In this study an experimental program is conducted to investigate the effects of fiber addition to concrete mixes on the mechanical properties of concrete, rebar corrosion resistance and sorptivity of concrete. For this purpose 0.45 water/cement ratio (w/c) concrete was produced with addition of steel, polypropylene or glass fibers into the casting mix at fixed volume fractions. Two different curing regimes were applied; curing in water tank and in laboratory conditions, were applied to the cast specimens.

Then, the fiber-reinforced concretes were tested to evaluate and compare their mechanical properties such as compressive strength, splitting tensile strength, rebound number, modulus of elasticity and flexure-toughness. Their performance was further investigated with respect to capillary surface rate of water absorption and accelerated corrosion testing involving impressed current initiated corrosion of concrete embedded reinforcement. Moreover, all test results were compared with the reference concrete containing no fibers.

The object of this thesis is to test the above mentioned concrete durability aspects on fiber reinforced concretes. An investigation of the effect of fiber reinforcement in concrete, on inhibiting the corrosion of reinforcing steel in concrete, as a result of improving durability performance of the concrete embedding the steel reinforcement. An attempt was made to investigate the ability to assess the durability of fiber reinforced concrete with their sorptivity coefficients and their mechanical properties which may indirectly provide insight to durability aspects.

ÖZET

LİF ÇEŞİTLERİNİN MEKANİK ÖZELLİKLER VE SÜREKLİLİK YÖNÜNDEN BETONARMEYE ETKİSİ

Bu çalışmada beton için elyaf eklemenin etkilerini mekanik özelliklerin üzerinde beton karışımı, rebar korozyon direnci ve beton geçirimini araştırmak için bir deney programı oluşturulmuştur. Bu amaçla 0,45 su / çimento oranı (w / c) olan; çelik, polipropilen veya cam elyaf katılmış beton üretilmiş ve sabit hacim oranlarıyla döküm için karışım hazırlanmıştır. İki farklı kür rejimi uygulanmış; su deposu olarak kür ve laboratuvar koşullarında, bu döküm örnekleri uygulanmıştır.

Daha sonra, lif eklemeli betonları değerlendirmek ve basınç dayanımı, ayrılma gerilme gücü, geri tepme sayısı, esneklik ve eğilme ve modül-dayanıklılık gibi mekanik özellikleri karşılaştırmak için deneyler yapıldı. Performansları, su emiş kapiler yüzey oranına ve gömülü takviyelerden geçirilen akıma dayalı hızlandırılmış korozyon testleriyle incelendi. Ayrıca, tüm test sonuçları lif içermeyen bir referans ile karşılaştırılmıştır.

Bu tezin amacı, yukarıda bahsedildiği gibi, lif takviyeli betonların süreklilik dayanımını test etmektir. Güçlendirilmiş betondaki lif takviyesinin, çeliklerin korozyonunu engelleyerek, dayanım performansını arttırmaya olan etkileri araştırılmıştır. Lif takviyeli betonun dayanım ve sürekliliğini araştırmak için, dolaylı olarak bir öngörü verebileceği için, betonun geçirgenlik katsayıları ve mekanik özellikleri kullanılmıştır.

TABLE OF CONTENTS

LIST OF FIGURES

LIST OF TABLES

LIST OF SYMBOLS / ABBREVIATIONS

a	width of specimen subjected to flexure, mm
A_{exp}	area of specimen exposed to water, mm^2
b	height of specimen subjected to flexure, mm
d	density of water, g/mm^2
D	cylinder diameter, mm
E_{OC}	initial balanced energy state
F	Faraday's constant
f_t	tensile strength, MPa
G_f	Fracture Energy, kg/sec^2
I_{aps}	Absorption
I	Current, Amp
I_1	initial current passing through the circuit, V
I_2	current passing through the circuit at first crack, V
I_N	toughness Index
L	cylinder length, mm
M	molar mass
m_t	change of specimen mass, grams
P	maximum applied load, N
Q	Electrical Charge, Amp.sec
R	Resistance, Ohm
R_1	reference resistance (11 Ohm)
R_C	concrete cover resistance
R_{corr}	concrete cover resistance increase caused by corrosion of the steel bar, Ohm
S	Sorptivity Coefficient
S_i	Initial Sorptivity
S_f	Final Sorptivity
t	time
V	Potential, Volt
V_1	initial potential measurement at the reference resistance
V_2	first crack potential measurement at the reference resistance

z	the number of electrons transferred

AR	alkaline resistant
CSH	Calcium Silicate Hydrates
FRC	Fiber-Reinforced Concrete
SFRC	Steel Fiber-Reinforced Concrete
GFRC	Glass Fiber Reinforced Concrete
PFRC	Polypropylene Fiber-Reinforced Concrete

1. INTRODUCTION

1.1. General

The use of fibrous reinforcement to enhance the properties of the cement matrix has gained broad recognition in recent years. Depending on the type of fiber, the fiber volume fraction and the way it is applied different fiber-reinforced concrete (FRC) characteristics can be achieved. Although the ability of fibers to enhance the mechanical properties of concrete is well established [1-4], there is still lack of a comprehensive, validated, and easily accessible database for the durability of fiber-reinforced concrete [5].

The first requirement for maximum durability against corrosion is low permeability concrete, with high cement content, a minimal chloride content and good cover to the reinforcing steel. Good quality concrete and good cover will increase the time needed for chlorides and carbonation to ingress to the reinforcing steel and initiate corrosion [6]. Long term performance will be affected by such factors as curing, compaction, and cover, but only to an extent that they influence either the porosity itself or the penetration depth necessary for corrosion to occur [7]. Crack formation and propagation may change the concrete composition and moisture level which will lead to deviation from the perfect diffusion equation [6], increase the rate of reinforcing steel corrosion and therefore, deteriorate the structure's integrity.

Since corrosion of steel in concrete is usually caused by the ingress of various agents (Cl^-, CO_2, H_2O, O_2, etc.) through the concrete cover, the measure of the permeation properties or the penetrability characteristics of concrete is important. Sorptivity, or capillary suction, is the primary mechanism of water and salt penetration under conditions of wetting and drying or partial immersion [7, 8]. Measurements will be strongly influenced by curing and environmental conditions, i.e. degree of saturation and temperature [6].

1.2. Scope and Objective

This thesis involves research and experimental studies on durability aspects of fiber reinforced concrete. Steel, glass and polypropylene fiber concrete behavior will be investigated and compared to regular concrete mixes. Fresh and hardened concrete properties will be considered, and further, experimenting with sorptivity measurements and accelerated corrosion techniques are attempted. Results obtained will be related to the contribution of fibers to initiation and propagation of concrete steel reinforcement corrosion and also initiation and propagation of cracks induced by corrosion.

1.3. Thesis Organization

Previous related research on fiber reinforced concrete (FRC) is presented in the Literature Review in Chapter 2. This chapter aims to provide a description of the mechanical properties of FRC based on previous studies and relate it to effects on FRC durability. Also included in this chapter is a description of the sorptivity test as a dominant water transfer mechanism in concrete cover. In Chapter 3, the Literature Review of the corrosion process and the corrosion-induced cracks of reinforcing steel in concrete are presented. This chapter also includes description and literature review of the impressed voltage accelerated corrosion test. In Chapter 4, literature significance is explained, therefore relating the previous research presented with the scope of this report. Chapter 5 describes the experimental procedure of the fresh and hardened concrete tests conducted, toughness, sorptivity and accelerated corrosion test. Chapter 6 contains an analysis of the experimental test results, a discussion of the results and a comparison to previous research. Chapter 7 summarizes the results from all conducted tests. Conclusions and recommendations are also given in this chapter. Details of each test and analytical results are provided in the appendices.

1.4. Research Significance

The slow process of corrosion of steel embedded in concrete may be accelerated by use of anodic polarization. It has successfully been used to model the real process of concrete reinforcement corrosion and study aspects like permeation characteristics of covercrete and corrosion resistance of concrete. Further, sorptivity of concrete has been proven to successfully investigate the transport mechanism of fluids in cover concrete and indicate the ability of concrete to absorb fluids from the environment into its pore system, therefore the ability of concrete to protect its embedded reinforcement from corrosion initiators.

The object of this thesis is to test the above mentioned concrete durability aspects on fiber reinforced concretes. An investigation of the effect of fiber reinforcement in concrete, on inhibiting the corrosion of reinforcing steel in concrete, as a result of improving durability performance of the concrete embedding the steel reinforcement. The effect of adding steel, polypropylene and glass fiber reinforcement to concrete is also studied on some properties of the concrete that closely relate to corrosion of reinforcing steel bars. These include water absorption and mechanical properties. An attempt is made to investigate the ability to assess the durability of fiber reinforced concrete with their sorptivity coefficients. Mechanical properties such as split-tensile strength and toughness may indirectly provide insight to durability aspects and also define the quality of the concrete.

Previous research upon this exact topic is very scarce. However, there is a well established database upon mechanical properties of various FRC, part of which can indirectly provide insight to the durability behavior, and scarce information on the direct influence of fibers to durability of concrete.

2. LITERATURE REVIEW ON THE ROLE OF FIBERS IN FIBER REINFORCED CONCRETE

2.1. Fundamental Principles of Fiber Reinforced Concrete

Fiber reinforced concrete is composed of hydraulic cements, aggregates and discrete reinforcing fibers. Fibers suitable for reinforcing concrete have been produced from steel, glass, synthetic materials and also from natural fibers [1, 3]. In Table 2.1 some typical properties of steel, glass and polypropylene fibers are presented. The concrete matrices may be cement mortars, normally proportioned mixes, or specifically formulated for a particular application, i.e. by adding to the casting mix corrosion inhibitors or water reducers. There are several ways fibers may contribute to cement-based fiber composite materials.

Fiber composites are developed to provide improved mechanical properties to otherwise brittle materials. When subjected to tension, concrete initially deforms elastically. The elastic response is followed by micro cracking, localized macro cracking and finally brittle fracture. The main concept of fiber reinforcement is to transfer the developed deformation of the brittle concrete matrix under load to the fibers as tensile stress, therefore taking advantage of the high fiber yield strain [4].

Introduction of fibers into concrete may result in post-cracking property changes that range from subtle to substantial, but for many practical aspects the matrix first crack strength (proportional limit) is not increased [1, 3, 4]. Fibers prevent large crack formation that can not only spoil aesthetics but also permit water and contaminants to corrode the steel reinforcement or deteriorate concrete. Nevertheless, the efficiency of fiber reinforced concrete depends upon a number of factors, including matrix strength, fiber type, fiber modulus, fiber aspect ratio, fiber strength, fiber surface bonding characteristics, fiber content, fiber orientation and aggregate size effects [1, 3].

Table 2.1. Typical Properties of Fibers [1]

Type of Fiber	Tensile Strength, MPa	Young's Modulus, GPa	Ultimate Elongation, %	Specific Gravity
Glass	1035-3795	70-85	2-5	2.50
Polypropylene	550-760	3.5-4.9	~25	0.90-0.91
Steel	275-2760	200	0.5-35	7.8

2.2. Steel Fiber Reinforced Concrete

2.2.1. Physical and Chemical Mechanism and Applications

SFRCs are cementitious materials reinforced with short steel fibers. The fibers are randomly distributed in the matrix to act as crack arresters.

Steel fibers have been used in concrete since the early 1900s. The early fibers were round and smooth and the wire was cut or chopped to the required lengths. The use of straight, smooth fibers has largely disappeared and modern fibers have either rough surfaces, hooked ends or are crimped or undulated through their length. Modern commercially available steel fibers are manufactured from drawn steel wire, from slit sheet steel or by the melt-extraction process which produces fibers that have a crescent-shaped cross section *(*see Figure 2.1). Carbon steels are most commonly used to produce fibers but fibers made from corrosion-resistant alloys are available. Stainless steel fibers have been used for high-temperature applications. Some fibers are collated into bundles using water-soluble glue to facilitate handling and mixing. Typically steel fibers have diameters from 0,15 mm to 2 mm and lengths up to 75 mm. Aspect ratios generally range from 30 to 100 [3].

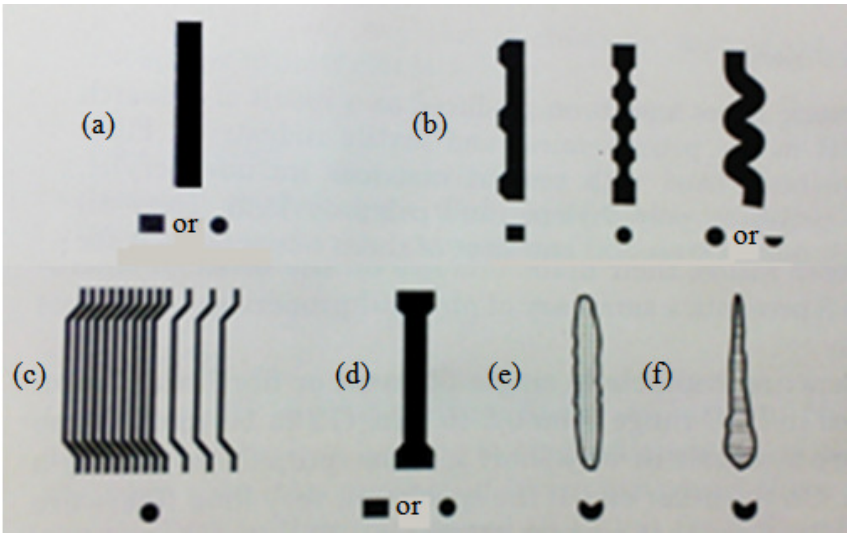

Figure 2.1. Various shapes of steel fibers used in fiber-reinforced concrete. (a) Straight slit sheet or wire (b) Deformed slit sheet or wire (c) Crimped-end wire (d) Flattened-end slit sheet or wire (e) Machines chip (f) Melt extract [3]

Steel Fiber Reinforced Concrete (SFRC) can be used when high tensile strength and reduced cracking are required, as well as the cases, when complex structural shapes are required, as a replacement of conventional steel reinforcement. Steel fibers have high tensile strength (275 – 2760 MPa) and modulus of elasticity (200 GPa), a ductile/plastic stress-strain characteristic and low creep. Usage of steel fibers considerably increases concrete toughness; the energy absorption capacity, offers more ductile behavior prior to the ultimate failure, reduced cracking, and improved durability [4, 9].

SFRC has a wide-range of applications such as; pavements and overlays, large industrial slabs, hydraulic and marine structures, dam constructions, repairing and retrofitting of reinforced concrete structures, tunnel linings and slope stabilization works and even conventional RC frames because of improved toughness against dynamic loads [3, 9]. Steel fibers have been used in conventional concrete mixes, shotcrete and slurry-infiltrated fiber concrete.

Typically, content of steel fiber ranges from 0.25 percent to 2 percent by volume. Fiber contents in excess of 2 percent by volume generally result in poor workability and fiber distribution, but can be used successfully where the paste content of the mix is increased and the size of coarse aggregate is not larger than about 10 mm.

2.2.2. Properties of Fresh SFRC and Workability

The most common control for quality assurance of fresh concrete is workability and air content. Further measures can be made for unit weight, concrete temperature, air temperature and relative humidity. Workability can be checked with the standard slump cone test (ASTM C143), with the V-B consistence test (BS1881, Methods of Testing Concrete, Part 2) or with the inverted slump test (ASTM C995). The inverted slump cone test is specifically developed for FRC to simulate the workability of vibrator compacted concrete. However, it is restrained to low slump, of maximum 10 cm slump, in which case the standard slump test is recommended [3].

Workability of concrete will decrease uniformly with the increase in fiber content. Generally, the addition of fibers make the mix stiffer. The addition of steel fibers at high dosages has potential disadvantages in terms of poor workability [1, 3, 10, 11]. Steel fiber aspect ratio also has significant influence on the workability of the fresh mix. Lower aspect ratio of fibers may result in higher compaction factors or lower inverted slump cone time and V-B test time. Also, the lower the aspect ratio of fibers, the lower the tendency they have to clump together. Shorter fibers achieve a more uniform dispersion within the concrete mix [10].

The need for using water reducing admixtures in the mix has become apparent for FRC, in order to improve workability without adding water. It has been proven that the addition of water reducing admixtures improves workability without having an adverse effect on the mechanical properties. High range water-reducing admixtures or superplasticizers can be used to obtain flowable concrete mixes even at a w/c ratio of 0.28 [3].

2.2.3. Properties of Hardened SFRC

The real advantage of using fibers in concrete can be seen after matrix cracking. The steel fibers, when homogeneously dispersed, act like small bridges and help for a

better distribution of tensile and shear stresses. So, the potential cracks in SFRC will be smaller in size and spread more evenly [9].

These types of materials are useful if a large amount of energy absorption capacity is required to prevent failure [3, 12].

Recent investigations indicate that an increase in the aspect ratio also increases the fracture energy of SFRC. Fracture energy of SFRC is proportional to the square of the length of fiber and inversely proportional to the square root of the fiber diameter. It has also been shown that hooked-end fibers give higher fiber pull-out loads than those of straight ones [12].

2.2.3.1. Compressive Strength. Effects of the fiber volume fraction and the fiber aspect ratio on the compressive strength and modulus of elasticity are not consistent. In [12] no significant change occurs when the fiber volume fraction is increased. In [9] compressive strength slightly decreases with increasing dosage of steel fibers (SFs). The diameter of the steel fibers and possibly their orientation may play a role in compression [12]. The addition of SF into concrete may have an effect of increasing the ductility in the compressive failure rather than the compressive strength itself [12].

2.2.3.2. Splitting Tensile Strength. In [3] it is reported that for cases with fiber volume fractions less than 2 percent the splitting tensile strength is not improved. In [12], experiments on concretes with water/cement ratios of 0.45 showed that the splitting tensile strength increases with increasing steel fiber volume fraction. For an aspect ratio of 65, an increase of the fiber volume fraction from zero (concrete without fibers) to 0.51 percent has resulted in an increase of 25 percent in corresponding splitting tensile strength, for the aspect ratios of 55 and 80, this increase was 21 percent and 15 percent, respectively. Concluding that more significant enhancements in the splitting tensile strengths can be found in SFRCs with the fiber aspect ratio of 65, particularly for the lower water cement ratios (i.e., w/c=0.45).

2.2.3.3. Modulus of Elasticity. In [1, 12] the modulus of elasticity slightly decreases with increasing dosage of SFs. In [13] the elastic modulus change with steel fiber addition and by increasing the fiber volume fraction is also insignificant.

2.3. Polymeric – Polypropylene Fiber Reinforced Concrete

2.3.1. Physical and Chemical Mechanism

Polypropylene (PP) fiber was first used in Portland cement concrete in the late 1960s [4]. Polypropylene is a synthetic hydrocarbon polymer, the fiber of which is made using extrusion processes by hot-drawing the material through a die. Polypropylene fibers are produced as continuous mono-filaments, with circular cross section that can be chopped to required lengths, or fibrillated films or tapes of rectangular cross section [14].

Polypropylene fibers are hydrophobic and therefore have the disadvantages of poor bond characteristics with cement matrix, a low melting point, high combustibility and a relatively low modulus of elasticity. Long polypropylene fibers can prove difficult to mix due to their flexibility and tendency to wrap around the leading edges of mixer blades [3].

The monofilament fibers have high elastic modulus and stiffness [14]. However, they have inherent weak bond with the cement matrix because of their relatively small specific surface area, whereas fibrillated polypropylene films have good fineness and dispersion so they can restrain the cracks in concrete at primary stage more effectively [1, 14]. Fibrillated polypropylene fibers are slit and expanded into an open network thus offering a larger specific surface area with improved bond characteristics. When the monofilament fiber content is high enough, it is similar to the function of steel fiber. Therefore, they can take more stress during destruction [14].

The most common application is on parts of the structure in tension when the concrete shrinks due to moisture loss. These stresses may exceed the concrete strength at early age leading to shrinkage cracks. Polypropylene and other synthetic fibers added to

concrete as secondary reinforcement have shown beneficial to control plastic shrinkage [15, 16].

Some researchers, however, suggested the reduction of aggregate content in order to increase the effectiveness of polypropylene fibers in concrete [1, 3].

2.3.2. Properties of Fresh Concrete and Workability

Generally, the addition of polymer fibers reduces the workability of the concrete [3]. The type and magnitude of the reduction depend on the fiber and dosage level. Microfibers can reduce the workability by drying out the mix due to their very high surface area to volume ratio [3]. In [17] an experimental research reports that fibrillated PP fibers have no effect on the workability and air content of fresh concrete at volumes below 0.3 percent, though an adverse effect on workability and an increase in air content of concrete resulted from 0.5 percent PP fiber volume.

Polypropylene fibers have been reported to reduce unrestrained plastic and drying shrinkage of concrete at fiber contents of 0.1 to 0.3 percent by volume [3]. Longer fibers have been reported to make finishing difficult as PP fibers tend to extend beyond the finished surface; however, they do not dry out the concrete mixture significantly [18]. Excessive fiber balling, even at higher volume fractions, is reduced resulting in better workability of the concrete mix containing shorter fibers [10].

In [8] it is proven that polymer fibers have a distinct impact on early age properties of concrete. At early age (before and shortly after the concrete sets), polymer fibers greatly improved concrete behavior, as: 1) slump was decreased (reducing movement of all types), 2) plastic shrinkage was greatly reduced, and 3) compression strength was increased, in comparison to normal concrete.

Polypropylene fiber contents of up to 2 percent by volume are claimed to have been used successfully with hand-packing fabrication techniques, but volumes of 0.1 percent of 5 mm fiber in concrete have been reported to have caused a slump loss of 75 mm [19].

In [11] it is reported that the addition of non-metallic fibers such as glass, polyester, polypropylene etc. result in better fresh concrete properties compared to SFRC regarding reduced early age cracking. This beneficial effect is attributed to their high aspect ratios and increased fiber availability (because of lower density as compared to steel) at a given volume fraction. Because of their lower stiffness, these fibers are particularly effective in controlling the propagation of micro cracks in the plastic stage of concrete.

2.3.3. Properties of Hardened Concrete

The effect of polypropylene fibers on the properties of hardened concrete varies depending on the type, length, and volume fraction of fiber, the mixture design, and the nature of the concrete materials used [15].

However, their effect on flexural, compressive and tensile strength as well as on toughness and elastic modulus is not clear. Most work shows either no effect or minor improvements in these properties [2, 15]. However, in some cases especially of fiber volume fractions of 0.5 percent or higher, the addition of polypropylene fibers decrease the ultimate strength of hardened concrete because of higher concentrations of entrapped air [3, 15].

Polypropylene fibers have a high tensile strength and high ultimate elongation, thus capable of large energy absorption, enhancing toughness and impact loading. Their high aspect ratio, due to their diameters that are in the order of micrometers, provides a very useful property for FRC [3]. However they are not known to significantly increase flexural strength [4]. The disadvantage of polypropylene fibers is their low elastic modulus [13, 15]. In general, while polypropylene fibers have shown little contribution to flexural strength, they have shown significant improvement in shrinkage cracking, impact resistance and ductility of concrete.

Polypropylene fibers are chemically inert and have relatively high tensile strength and an acceptable resistance to temperature (165°C average melting point and 130°C average for highest safe temperature). [13, 15]. It has been shown that their major

contribution to fiber reinforced concrete is due to their micro crack-arresting capabilities [11].

2.3.3.1. Compressive Strength. Polypropylene fibers are not known to significantly alter compressive strength of concrete [3]. In [17] PP fibers had a relatively small favorable effect on compressive strength of concrete when 12 mm long fibers were used.

2.3.3.2. Tensile Strength. Previous research derived that PFRC tensile strength is maintained at the same levels as in unreinforced concrete or slightly enhanced [3].

2.3.3.3. Modulus of Elasticity. No significant effect on the modulus of elasticity of concrete is known to be produced by addition of PP fibers [2, 15].

2.4. Glass Fiber Reinforced Concrete

2.4.1. Physical and Chemical Mechanism

Glass fiber is available in continuous or chopped lengths. Fiber lengths of up to 35 mm are used in spray applications and 25 mm lengths in premix applications.

Glass fibers are high modulus; high strength and can improve strength and toughness characteristics of concrete by reducing the crack propagation [4]. Glass fiber has high tensile strength (2 – 4 GPa) and elastic modulus (70 – 85 GPa) but has brittle stress-strain characteristics (2 – 5 percent elongation at break) and low creep at room temperature. Claims have been made that up to 5 percent glass fiber by volume has been used successfully in sand-cement mortar without balling. Glass fibers are sensitive to corrosion at high stress levels and may have problems with relaxation. Also, it has been proven that different lengths of fibers would control different scales of cracking [11].

Alkali-resistant glass fiber is used in the manufacture of glass-reinforced cement (GRC) products, to resist deterioration caused to glass in the concrete alkaline environment [20, 21]. Widespread development of glass fiber reinforced concrete (GFRC) has resulted from the development of alkali-resistant glass containing high percentages of zirconia. It was successfully formulated in the 1960s and by 1970 it was in commercial production in Britain and USA [22, 23]. GFRC was initially confined to non-structural uses where it had wide applications in direct spray techniques and premix processes and replaced the asbestos fiber in a variety of precast products. However, by this time GRC products are used extensively in construction in agriculture, for architectural cladding and components, and for small containers.

2.4.2. Properties of Fresh Concrete and Workability

In [11] results show good fresh concrete properties and reduced early age cracking. In [16, 17] a decrease in mix workability by means of reduced slump was observed with glass fiber addition.

2.4.3. Properties of Hardened Concrete

2.4.3.1. Compressive Strength. Previous research derived [16, 20] GFRC compressive strengths to be maintained to the same levels of unreinforced concrete or slightly enhanced. Also, in [24], it is proved that the higher the tensile strength of the fibers the better the compressive strength of the GFRC.

2.4.3.2. Tensile Strength. Previous research derived that GFRC tensile strength is maintained at the same levels as in unreinforced concrete or slightly enhanced [16, 20].

2.4.3.3. Modulus of Elasticity. Glass fiber addition to concrete may increase the modulus of elasticity but the increase has not been proven significant [3, 25].

2.5. Flexure and Toughness of Fiber Reinforced Concrete

The most notable improvement of the mechanical characteristics of FRC in comparison to unreinforced concrete is FRCs superior fracture resistance [26]. The flexural strength is also enhanced with the incorporation of fibers. Strength and toughness are two mechanical performance parameters presently being used in design specifications. Toughness is a measure of the energy absorption capacity of a material and is used to characterize the material's ability to resist fracture when subjected to static strains or to dynamic or impact loads.

The flexural strength of FRC may be determined under three-point loading using ASTM C 1018, or by center-point loading using ASTM C 293. Maximum flexural strength is calculated at the section of maximum moment corresponding to the peak fiber stress in tension based on the assumption of elastic behavior, as shown in Figure 2.2. The relationship between flexural strength and tensile strength has not been determined for FRC. Direct tension tests on FRC are difficult to be conducted, so the flexural test is recommended for determining the toughness of FRC [2].

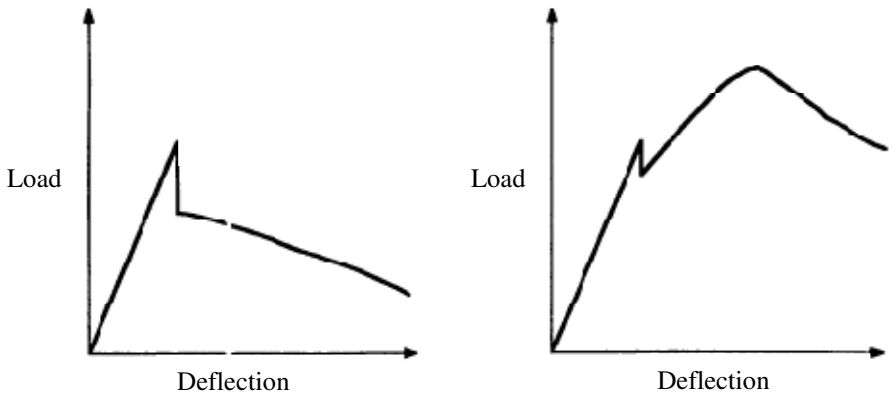

Figure 2.2. Flexural strength – Calculated in accordance with ASTM 78 or C 293 using the maximum load [2]

Test standards for measurement of toughness include the most popular ASTM C 1018 and JSCE-SF4. There are some contradictions regarding how these indices should be measured, interpreted and used. In [26, 27] the differences between these test methods and their toughness evaluation capabilities and drawbacks are studied. In ASTM C 1018 it is proposed to evaluate the toughness indices and in JSCE-SF4 it is recommended to determine the flexural toughness factor.

According to [28], RILEM was the first to establish a standard test procedure for evaluating toughness of FRC capable of taking into account the post cracking behavior in 1985. In order to adjust a three-point bending test to take account of the fracture process zone and evaluate fracture energy, the concept of fracture energy (G_f) is considered [28]. Also several attempts [26, 27, 28] have been made to derive an effective fracture-toughness test procedure, mainly with steel fiber reinforced concrete. However, each test is useful for comparing relative performances of different concrete mixes and for providing information on strength and toughness [26].

2.5.1. Steel Fiber Reinforced Concrete

High modulus and high strength steel fibers can improve strength and toughness characteristics of concrete acting as crack arresters, mainly restricting the crack propagations [4, 11]. For higher fiber content, longer fibers and higher values of aspect ratio, larger toughness values are obtained, indicating the effective contribution of steel fibers to concrete toughness [3, 29, 12]. The orientation of the fibers can considerably influence the post-cracking resistance of concrete [10]. Higher fiber contents result in much higher load-retaining capacity at large deflections [30]. This is particularly true for hooked-end fibers. For hooked-end fibers the length of fibers does not affect toughness significantly [30]. Hooked ends form mechanical anchors in concrete upon deflection, consequently increasing the fiber pullout load. In [9] SFRC crack propagation was restrained by the fibers and the sample did not break into pieces at the ultimate load, but the terminal stresses seemed to be distributed all over.

2.5.2. Polypropylene Fiber Reinforced Concrete

Polypropylene fibers have shown to improve flexure capacity [11]. This benefit is attributed to their high aspect ratios and increased fiber availability (because of lower density as compared to steel) at a given volume fraction. PP fibers in [25] are proven to provide an improvement of the resistance to fracture in various tested mortars [25]. Because of their lower stiffness, these fibers are particularly effective in controlling the propagation of micro cracks in the plastic stage of concrete. Fibrillated polypropylene fibers could result in a better post-peak performance than single strand fibers. However, their contribution to post-cracking behavior, unlike steel fibers, is not known to be significant [11]. Polypropylene fibers are tough but have low tensile strength and modulus of elasticity. In [17] it is reported that, for volumes equal to or less than 0.3 percent, 18 mm long fibers were more favorable for enhancing the post-peak resistance.

2.5.3. Glass Fiber Reinforced Concrete

As with polypropylene fibers, glass fibers are proven beneficial in flexural and tensile behavior, due to their high aspect ratios and increased fiber availability (because of lower density as compared to steel) at a given volume fraction [11, 31]. Because of their lower stiffness, these fibers are particularly effective in bridging the propagation of micro cracks in the plastic stage of concrete. However, their contribution to post-cracking behavior, unlike steel fibers, is not significant. Derived in [11] it is shown that the inability of glass fibers to sustain high crack widths resulting at large deflections causes the post-peak performance to be poorer compared to individual steel fiber concrete.

Other studies on GFRC [16, 20] report a first crack flexural strength increase up to 3 times the strength of un-reinforced concrete, but with increasing fiber volume content the rate of strength increase tends to decrease, possibly because of difficulty achieving uniform fiber distribution. At 0.5 percent fiber content the flexural strength increased with increasing lengths. The ultimate flexural strength also increased up to 5 times the unreinforced concrete but, again, with increasing fiber volume content the rate of strength increase tends to decrease. In [11] glass fibers performed worse than steel and

polypropylene fibers, with respect to toughness (primarily, post-peak) owing to their weakness of getting pulled out because of their short lengths.

2.6. Effect of Fibers on Durability of Concrete

2.6.1. Introduction

Limited research is available on the durability aspects of fiber reinforced concrete. Corrosion, as will be described in chapter 3 of this report, is the biggest durability problem in construction. Possible positive contributions of fibers to FRC durability may be by delaying the corrosion process of embedded steel reinforcement [32].

The effect of fibers to durability aspects of concrete may be attributed to the durability aspects of the fibers themselves, to their interaction with cement in short and long term periods and to their concrete engineering property enhancements. Some important fiber durability concerns and the physical and chemical interaction of fibers with the concrete mix are investigated within this chapter.

Also, as concrete steel reinforcement corrosion process, the most important durability problem, is closely related to the cover permeation characteristics, a description of the transport mechanism of ions and fluids within concrete is presented. It is considered necessary to investigate the effects of fibers to these transport mechanisms that are closely related to the corrosion process.

2.6.2. Fiber Durability Aspects

2.6.2.1. Corrosion of Steel Fibers. Corrosion of fibers can be limited to the surface skin of the concrete and will not propagate more than 2.5 mm [1]. In a well-compacted concrete with 28 day compressive strength over 21 MPa with w/c complying with ACI 318,

corrosion propagation is restrained as there is no continuous conductive path for stray or induced currents or currents from electromotive potential between different areas of the concrete [1]. However, if SFRC is needed for uses where cracks may be expected, corrosion of carbon steel fibers bridging the cracks will occur to some extent and will most possibly affect their properties.

2.6.2.2. Glass Fibers. Durability of glass fibers in the concrete alkaline environment is a major concern. Despite the use of improved alkaline-resistant glass fibers (AR-glass) and addition of pozzolanic materials such as silica fume and fly ash, aging problems still occur [3, 20-23, 31]. The long-term properties of glass fiber reinforced cement (GFRC) composites have shown a reduction in strength and ductility with time [31]. Aging of GFRP deteriorates the glass fibers. The reasons for this are not clear and it is speculated that alkali attack or fiber embrittlement are possible causes. The cement hydration in GFRC composites, immersed in water or exposed to weathering, results in lime crystals and calcium silicate hydrates (CSH) penetrating the fiber bundles, filling the interstitial spaces between glass filaments, thereby increasing the bond to individual glass filaments (embrittlement) [23, 31]. In [31] it is indicated that the blended cement consisting of a specific synthetic pozzolan, metakaolin, significantly improves the long term properties of GFRC composite.

2.6.2.3. Polypropylene Fibers. Polypropylene fibers can be assumed to have long term durability. Polypropylene fiber reinforced concrete (PFRC) subjected to flexural strengths after various aging periods have shown an increase in strength. Fibers not only did not deteriorate but also bonded well within the matrix to provide an enhanced post crack resistance. The increase is assumed to be caused by better bonding achieved as cement hydrates continuously with age [3]. There is no concern about the alkaline environment in Portland cement [3].

Polypropylene fibers mitigate plastic and early drying shrinkage by increasing the tensile concrete and bridging the forming cracks [13, 15, 16].

In [15] it is proven that permeability, abrasion and impact resistance of concrete are all significantly improved by the addition of polypropylene fibers. But in [13] the incorporation of polypropylene fibers increased the permeability of plain concrete. This is attributed to the fact that polypropylene fibers increase the void content in plain concrete due to the lack of cohesiveness of the cement matrix and poor dispersion of fibers. With increasing fiber length from 12.5 mm to 19 mm, concrete specimens exhibited an increase in permeability.

The effect of polypropylene fiber reinforcement is more intense in Portland mortars than in alkaline ones. Polypropylene fibers experience superficial alterations within alkaline media, especially at high temperature. These alterations can affect the adherence to the matrix and therefore deteriorate the PFRC [3, 25].

2.6.3. Concrete Cover Penetration Mechanism

Concrete properties such as strength, durability and permeability are directly influenced and controlled by the number, type, size and distribution of pores present in the cement paste, the aggregate components and the interface between the cement paste and the aggregate. For example, strength and elasticity of the concrete are affected by the total volume of pores whereas permeability is influenced by the pore size distribution and continuity. It is believed that capillary voids larger than 50 nm, produce negative effects to strength and impermeability. The water existing in pores larger than 50 nm plays an important role in the durability of concrete [33].

Capillary absorption, hydrostatic pressure, and diffusion are the means by which chloride ions or other deleterious agents can penetrate concrete. First, diffusion is the process by which agents are transported from a part of the concrete to another due to a concentration gradient. The progress of diffusion in concrete is very slow and it occurs as a result of small random molecular motions over small distances [33 - 35].

The second mechanism for chloride ingress is permeation. Permeability is a concrete property that has been studied extensively, however many times referring to the

general penetrability of concrete, regardless of the transport mechanism. For permeation to exist there is need for an applied pressure. If there is an applied hydraulic head on one face of the concrete and aggressive ions or liquids are present, they may permeate into the concrete. Permeability increases in existence if high porosity or cracking which facilitates the ingress of water, chlorides, and other corrosive agents [33, 36, 37].

A more common transport method is absorption. It is defined as the transport of liquids in porous solids due to surface tension in capillaries. As a concrete surface is exposed to the environment, it will undergo wetting and drying cycles. When water encounters a dry surface, it will be drawn into the pore structure through capillary suction. Absorption is driven by moisture gradients. **S**orptivity, a common measurement for the rate of absorption or capillary suction, is the primary mechanism of water and salt penetration under conditions of wetting and drying or partial immersion [7, 33].

Of the three transport mechanisms described above that can allow deleterious substances to initiate the concrete rebar corrosion, the principal methods are diffusion and absorption. It is rare for a significant hydraulic head to be exerted on a structure. In the bulk of the concrete, the pores remain saturated and chloride ion movement is mainly controlled by concentration gradients. The effect of absorption is typically limited to shallower penetration depths in the surface region of concrete. Although many absorption tests have been used for laboratory and field measurements [35], sorptivity was selected as the most appropriate for the scope of this report.

2.6.4. Sorptivity

Sorptivity is defined as '*the rate of absorption of water into an unsaturated surface of concrete by capillary action*' of concrete's pore structure [38]. It was first carried out by Hall in 1989 who named it water sorptivity. It is the governing mechanism controlling rates of water ingress into unsaturated or partially saturated concrete.

For one dimensional flow, it can be stated that [38]:

$$I_{abs} = S\, t^{\sqrt{2}} \qquad (2.1)$$

where I_{abs} is the cumulative water absorption per unit area of inflow surface, measured in mm, S is the sorptivity and t is the elapsed time. The absorption, I, is the change in specimen mass divided by the product of the cross-sectional area of the exposed surface and the density of water, as expressed by Equation 2.2 [39].

$$I_{abs} = \frac{m_t}{A_{exp}/d} \qquad (2.2)$$

where m_t is the change of specimen mass in grams, at the time t, a is the exposed area of the specimen, in mm^2, and d is the density of water in g/mm^2. The rate of water absorption ($mm/s^{1/2}$) is defined as the slope of the line that is the best fit to I plotted against the square root of time ($s^{1/2}$) [39].

When dry concrete is initially exposed to water, it will absorb water following Equation 2.1 with some initial sorptivity, say S_i. After some time there will be a change from this value and then the additional absorption will follow the same relation with another sorptivity, S_f. This change has been attributed to the initial dominance of the larger capillary pores resulting in a larger sorptivity value until they are filled, after which the smaller gel pores dominate with their lower sorption effects.

Concrete sorptivity or a concrete surface water absorption may depend on many factors from the below enlisted [39]:

- concrete mixture proportions;
- the composition and physical characteristics of all components of the concrete;
- the presence of chemical admixtures and supplementary cementitious materials;
- the entrained air content;

- the type and duration of curing. Also, the degree of hydration together with the age of the concrete. Water absorption is also strongly affected by the moisture condition of the concrete at the time of testing;
- the presence of microcracks;
- the presence of surface treatments such as sealers or form oil [40]; and
- placement method including consolidation and finishing.

In [40] it is shown that the sorptivity coefficient of concrete is very sensitive to the curing conditions. The effect of curing condition on the sorptivity coefficient of concrete seems to be higher in low-strength concretes. Also in [40] it is proven that the sorptivity coefficient of air cured concrete samples decreases as the compressive strength of concrete increases. However not for concrete cured in water for 28 days, where the sorptivity coefficient is kept constant for increasing compressive strength.

2.6.5. Fiber Effect on Concrete Cover Penetration

The addition of fibers to a concrete mix may alter the penetrability of the concrete surface. Concrete permeation characteristics' alteration by adding fibers will show the effect fibers may have to the initiation of corrosion.

Reports in [3] mention several parameters that could affect the durability performance of FRC. The fiber stiffness, the fiber length and fiber content, the water absorption ability of fibers and the fiber-concrete bond characteristics may affect the FRC stiffness and permeability properties. Fibers existence in a concrete mix is expected to reduce penetrating paths formed by the pore system. They may act as pore blockers and change the water, oxygen or chloride concentrations within concrete.

Reinforcing fibers significantly reduce the water permeability at post cracking, by restraining the formation of cracks. Fibers in concrete reduce the flow rate at a given crack width and increase the critical crack width below which no further flow occurs [41]. In bending, failure is caused in tension and is governed by the largest crack in the specimen. With increased porosity, the maximum crack size is also likely to increase [41]. However,

for the propagation of a single crack, bridging stress provided by fibers is effective in delaying ultimate failure. The flexural strength and toughness of FRC can validate the fiber concrete bond characteristics and therefore provide an insight about concrete cover penetration.

2.6.5.1. Steel. Due to the high stiffness of steel fibers, micro-defects such as voids and honeycombs could form during placing as a result of improper consolidation at low workability levels [11].

Also an indirect positive effect towards cracked SFRC durability would come from increased tensile strength, which would withstand the propagation of corrosion induced cracks more effectively. This could increase the lifetime of a structure.

2.6.5.2. Glass. Limited available research on GFRC provides indications that factors such as fiber water absorption and stiffness could have effect on the GFRC penetrability. Generation of voids due to stiff fibers mixed in concrete increases the risk of higher air content and higher porosity of the GFRC but on the other hand higher glass fiber water absorption may allow the fibers to mix more homogeneously within the cement. Furthermore the glass fiber tensile strength may influence the durability of concrete, clearly by increasing crack resistance.

2.6.5.3. Polypropylene. Limited results available generally indicate that the permeability of polymeric fiber-reinforced concrete and plain concrete are about the same. However, some contradictory results have been reported upon the durability of PFRC.

In [17] it is obtained that fibrillated PP fibers tend to increase permeability of concrete. With 6 mm long fibers, the increase was relatively mild but with 18 mm long fibers the permeability increase was significant. Similarly, in [13] it was found that reducing fiber length from 19 mm to 12.5 mm, with an equivalent volume fraction, resulted in a decrease in the permeability of concrete.

In [19] polypropylene fiber reinforced concrete (0.2 percent) slabs of different w/c of 0.45, 0.55 and 0.65 were subjected to severe corrosion initiating conditions and their resistance to corrosion was monitored for a period of more than 7 months. The results indicate polypropylene fiber reinforcement has no noticeable effect in delaying corrosion of reinforcing steel in concrete.

However, in contrast to the above, [42] indicates a high reduction of the permeability of concrete due to the addition of polypropylene fibers. By using the Von test method a reduction of the order of 44 to 70 percent was measured by using different mixes. In [32] it is recommended that a method that can potentially decrease permeability is the addition of polymer fibers and in this way initial chloride intrusion could be minimized.

In [43] experiments on 0.5 w/c polypropylene fiber reinforced concrete with fiber content 0.5 percent by volume focused on crack control and report a reduced corrosion rate of embedded reinforcement, in comparison to concrete without fibers.

3. LITERATURE REVIEW ON THE CORROSION OF STEEL BARS IN CONCRETE

The dissolution of iron due to corrosion and subsequent formation of corrosion products results in a volumetric expansion [6, 34]. Full corrosion process leads to a volume increase at the steel-concrete interface of two to ten times [6]. As corrosion progresses and more and more corrosion products are formed, major stresses are developed within the concrete structure [44]. Once the tensile strength of the concrete that surrounds the reinforcement is surpassed, it will crack [34].

Reinforcement corrosion is a slow process, usually easy to detect before catastrophic failure [6]. But cracking of the concrete cover will ultimately result in spalling or delamination of the deck surface [6, 34, 44]. In case of concrete cover spalling it may even have tragic consequences, i.e. large pieces of concrete have fallen of bridges causing fatalities [6].

For this ultimate spalling to occur there is need for two phases of the corrosion process to conclude. Firstly, the initiation of corrosion, which includes the depassivation and the actual initiation of corrosion, and then the propagation of corrosion by means of continuously increased internal stresses producing cracks capable of fracturing the concrete cover [44, 45]. Different parameters may influence these phases.

3.1. Process of Corrosion

Corrosion is an electrochemical process involving reactions between steel, concrete and the environment that they are contained in. For corrosion to take place the steel bar reinforcement will act as an anode and as a cathode. It will connect these two regions which can be at adjacent parts of the steel (micro-cell), or at distant places of the same bar, usually at different local environmental conditions (macro-cell). Figure 3.1 below gives a schematic illustration of reactions involved for corrosion to take place on concrete

reinforcing steel bars. The end product of the corrosion process on the rebar and at the steel concrete interface is hydrated ferric oxide ($Fe_2O_3.H_2O$), commonly known as rust, (see equations 3.1 - 3.5), forming in the anode.

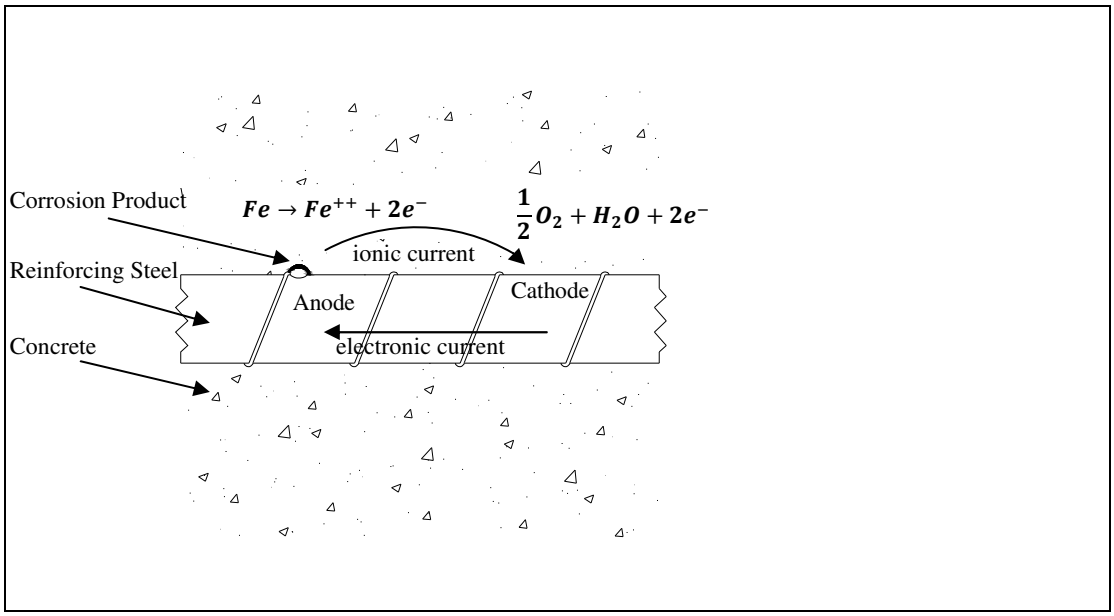

Figure 3.1. Schematic representation of the corrosion of reinforcement steel in concrete

The anodic reaction (dissolution of steel/iron):

$$Fe \rightarrow Fe^{++} + 2e^- \tag{3.1}$$

Another anodic reaction that may promote the corrosion initiation by depletion of the alkalinity in the vicinity of the anodic areas is the anodic reaction of oxygen evolution [46]:

$$2H_2O \rightarrow O_2 + 4H^+ + 4e^- \tag{3.2}$$

Alkaline ions in the pore solution and alkaline concrete constituents like calcium hydroxide may be neutralized by acidity produced by this reaction.

At the cathode oxygen is reduced to form hydroxyl ions, consuming the electrons supplied from the anode. The cathodic reaction:

$$\frac{1}{2}O_2 + H_2O + 2e^- \rightarrow 2OH^- \tag{3.3}$$

Further reactions at the anode following the steel dissolution:

$$4Fe^{++} + 2OH^- \rightarrow Fe(OH)_2 \tag{3.4}$$

$$4Fe(OH)_2 + O_2 + 2H_2O \rightarrow 4Fe(OH)_3 \rightarrow 2Fe_2O_3.H_2O + 4H_2O \tag{3.5}$$

The hydroxyl ions migrate through the solution (electrolyte) to the anode where they combine with the metallic ions released by the anodic reaction to form iron oxides. One possible is the formation of Fe_2O_3, which is the 'brown rust' ferrous oxide compound. The oxygen availability at this stage influences the reaction and in case of restricted oxygen supply the product could be Fe_3O_4.

3.2. Corrosion of Steel in Concrete

3.2.1. Passivity

Concrete embeds steel and provides a physical barrier and chemical protection against corrosion [6]. Portland cement concrete pore solution that is not exposed to any external effects usually has a pH between 12 and 13 [6]. The Pourbaix diagram (Figure 3.2), defines the ranges where passivity, immunity and corrosion may exist depending on the electrode potential and the pH [47]. Considering the H_2O - Fe system in the concrete alkaline environment and at the potentials normally existing in the concrete, it can be noticed that our system normally begins its lifetime in a state of passivity.

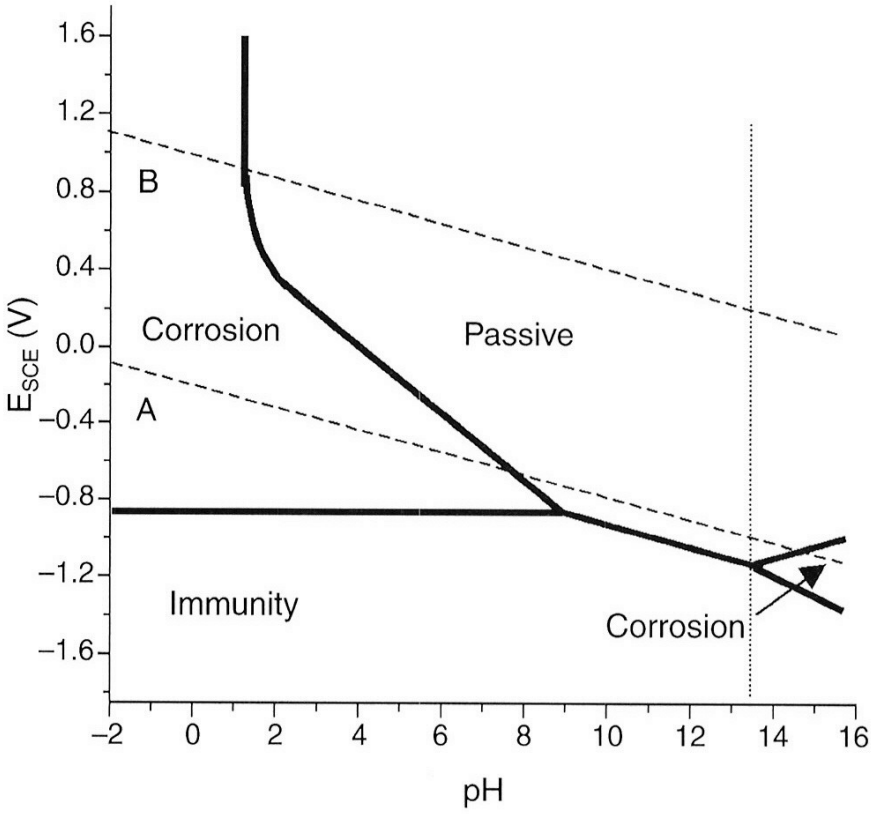

Figure 3.2. Pourbaix diagram for $Fe\text{-}H_2O$ at 25°C [48]

Steel, as most metals, exposed to atmosphere tends to revert to its natural state, at a lower energy level, which is oxide or hydroxide. In physical terms, for steel in concrete, this means that a tight, ultra thin (<10nm) protective layer of insoluble products, oxide or hydroxide (e.g. Fe_2O_3) adheres over the surface of steel, restraining further anodic steel dissolution [6, 47].

This 'natural protection' against corrosion of steel in concrete comes as great relief to engineers; however it may take years to form and also, it is proven to be terminated in long term uses. As a result of reduction of the protective nature of the passive layer, active corrosion of steel in concrete is allowed to initiate. Chloride ion attack, mostly from de-icing salts or seawater, penetrating into the concrete surface and carbon dioxide, from the atmosphere, are two major factors that can break the passive film on the surface of steel and initiate corrosion.

3.2.2. Corrosion Initiation – Carbonation and Chloride attack

3.2.2.1. Carbonation. Carbonation is the result of the interaction of carbon dioxide gas (CO_2) in the atmosphere with the alkaline hydroxides in the concrete [6]. Like many other gases carbon dioxide dissolves in water to form carbonic acid. Unlike most other acids the carbonic acid does not attack the cement paste, but just neutralizes the pH in the pore water, mainly forming calcium carbonate that lines the pores.

$$CO_2 + H_2O \rightarrow H_2CO_3 \tag{3.6}$$

$$H_2CO_3 + Ca(OH)_2 \rightarrow CaCO_3 + 2H_2O \tag{3.7}$$

There is a lot more calcium hydroxide in the concrete pores than can be dissolved in the pore water. This helps maintain the pH at its usual level of around 12 or 13 as the carbonation reaction occurs. However, eventually all the locally available calcium hydroxide reacts, precipitating the calcium carbonate and allowing the pH to fall to a level of less than 8, over passing the steel corrosion threshold pH value of 11, where steel will corrode.

3.2.2.2. Chloride attack. Chloride attack of reinforcement by diffusion of chlorides into the concrete cover is the other major corrosion problem met. The initial mechanism appears to be suction, especially when the surface is dry. Salt water is rapidly absorbed by the dry concrete. There is then some capillary movement of the salt-water through the pores followed by diffusion. Chloride diffusion produces a concentration level rather than a ‘front’. The chloride ions attack the passive layer without affecting the concrete pH. Chlorides act as catalysts to corrosion when there is a sufficient concentration at the rebar surface to break down the passive layer of oxide on the steel and allow the corrosion process to proceed quickly. Nevertheless, chloride concentration may be too low to break down the passive layer, especially as it has the ability to reform itself. A ‘chloride threshold’ value, given in terms of the chloride hydroxyl ratio, which if achieved, corrosion will initiate has been studied in [49].

3.2.3. The influence of concrete properties on rebar corrosion

As described, chloride ions or carbon dioxide penetrate the concrete cover depth to reach the surface of the reinforcing steel by a number of mechanisms. The concrete cover should be adequate to resist these penetrating mechanisms. Several factors may influence the quality of the cover.

Increased cover thickness provides longer penetration path and therefore inhibits corrosion. But the increased cover thickness also produces more bleeding and higher risk of shrinkage cracking formation which will counteract corrosion protection by allowing easier access of deleterious agents [50]. So the quality of the cover is important and also the rate of agent ingress should be considered rather than the length of the path to steel reinforcement. The rate of ingress and the penetrability of corrosion agents into concrete clearly depend on the pore structure of the concrete. Therefore the factors that influence the pore structure are to be considered.

Two factors that significantly influence capillary porosity in concrete are the water to binder (w/b) ratio [6, 49] and the use of supplementary cementing materials [51, 52, 53]. A w/b ratio of 0.42 or higher is required for the complete hydration of cement. However, hydration is a gradual process and the unused mixing water is retained in the capillary pores. Higher w/b ratios, used to give a workable mixture, increase the amount and interconnectivity of capillary porosity in the cement paste allowing greater penetrability. With the introduction of high range water reducing agents, w/b ratios as low as 0.38 are possible and significantly limit the penetration of chloride ions and carbon dioxide [52].

Curing of concrete is a parameter of major importance that can change the penetrability of chloride ions and carbon dioxide into the concrete [54]. Better curing causes lower permeability, better hydration, more CH and consequently, less carbonation and chloride diffusion. High-temperature curing of concrete accelerates the curing process so that at early ages, a high-temperature cured concrete will be more resistant to aggressive ion penetration than a normally-cured concrete at the same at age [55].

Another influence on the pore structure is from the environmental conditions at early age of concrete. Temperature, relative humidity, wind and direction of sunlight, and

the type of environment (e.g. pollutant and coastal regions) are the other effective factors [50, 54, 55]. The older the concrete, the greater amount of hydration that has occurred and thus the more highly developed will be the pore structure [54].

3.3. Accelerated Corrosion Technique

Under natural conditions the process of reinforcement corrosion is very slow; usually the first crack observed on the outer concrete surface appears after many years. Acceleration of the corrosion process can be accomplished by applying a constant potential (potentiostatic) or an electric current of constant magnitude (galvanostatic) between the embedded steel and another electrode placed outside the concrete specimen acting as a cathode. Accelerated corrosion by means of the impressed voltage or current techniques is widely used in concrete durability tests [56 - 58].

The impressed voltage technique indirectly gives information about the permeation characteristics of concrete. Improved permeability characteristics of concrete delays the initial corrosion time and increases the resistance to corrosion cracking, by decreasing the corrosion rate [56, 57].

This method differs to the common causes of corrosion initiation in the fact that a closed electric circuit is formed within which the concrete cover acts like the resistor. Ohms' Law applies as with common electric circuits (Eqn. 3.8).

$$V = I \cdot R \tag{3.8}$$

where I is the current in amperes, V is the potential difference in volt, and R is the circuit resistance measured in Ohm.

By applying a constant voltage or current DC to the reinforced concrete specimen, with an initial balanced energy state (E_{OC}), the specimen will be polarized. Connecting the steel rebar to the positive pole anodically polarizes the steel by means of a counter-

electrode. When steel embedded in concrete is anodically polarized various anions in the cover, e.g. chloride, will migrate to the steel surface and initiate the corrosion process, and simultaneously cations, (iron, etc.) will migrate to the outer surface of the mortar specimen [57, 58]. The migrations of ions in mortar can change the concrete microstructure and some properties of the cover. But, this method possibly modifies the corrosion process and the corrosion pattern due to iron migration in concrete pores [57].

During this test all stages of corrosion process are involved. Potential drop V is measured between the embedded reinforcement bar and the external counter-electrode. As the current density value is constant, the potential V is proportional to an electrical resistance R of the medium between reinforcing steel and counter-electrode. Expansion of the concrete cover starts only after the pores close to steel are completely filled with corrosion products.

Keeping the test specimen and the cathode inside a solution, containing electrolyte such as salt, can further accelerate steel corrosion [6]. In the tests conducted in [57] it was observed that the presence of chlorides in the solution, further accelerated crack initiation. In fact, passivity of steel in an alkaline and chloride-free concrete cover provides resistance to stray currents [46]. Also, corrosion products exerting to the concrete surface in [30] were of different color, depending on the presence or absence of chlorides in the solution. For samples tested in chloride containing solution, green rust appears on the concrete surface at the point of first recorded volume expansion, though prior to cracking. And at cracking, cracks appeared filled with green rust which gradually became red. In absence of chloride a white product appeared on the concrete surface and cracking was comparatively much delayed.

A reduced amount of dissolved oxygen in the solution can inhibit corrosion, though many other reduction parameters can consume the electrons [6]. It should also be noted that a higher ionic conductivity of the cover, with all its components, would easier allow corrosion reactions to take place.

Where an impressed current is used for corrosion process, the steel mass loss is related to the electrical energy consumed once passivity has been compromised [48]. Their relationship is expressed using Faraday's law:

$$Mass\ loss = \frac{Mit}{zF} \tag{3.9}$$

where M is the molar mass (55.847 g/mol for iron); i is the current (Amp.); t is the time (sec); z is the number of electrons transferred; and F is Faraday's constant (96,4877 Coulomb/mole).

Previous experiments have shown that a level of current density above 200 $\mu A/cm^2$ results in a significant increase in the strain response and crack width due to corrosion of the steel reinforcement [58]. The electrical resistivity values of the fibers used in this study produce a significant scatter, therefore it is necessary to consider electrical resistivity of the concrete cover constituents as a parameter that may alter the circulation of current and the rebar corrosion process in the accelerated corrosion test. Table 3.1, below, presents the electrical resistivity values of relevant materials.

Table 3.1. Electrical Resistivity Values for Relevant Materials [59]

Material	Electrical Resistivity (Ω-m)
Steel	$\sim 10^{-7}$
E-Glass	4×10^{14}
Polypropylene	$>10^{14}$
Concrete (dry)	10^{9}

The results of [58] showed that, up to 7.27 percent mass loss was effective in inducing corrosion of the steel reinforcement in concrete, using accelerated corrosion impressed current technique. These tests involved variation of the current density and it was proved that the use of different current densities has no effect on the percentage of mass loss.

4. EXPERIMENTAL STUDY

In this study an experimental program was conducted to investigate the effect of fiber addition to concrete mixes on the mechanical properties of concrete, on the rebar corrosion resistance and on the sorptivity of concrete. For this purpose, 0.45 w/c concrete was produced with addition of steel, polypropylene or glass fibers into the casting mix, at fixed volume fractions. Two different curing regimes were applied to the cast specimens, curing in a water tank or curing in laboratory ambient environmental conditions.

Then, the fiber-reinforced concretes were tested to evaluate and compare their mechanical properties such as compressive strength, splitting tensile strength, rebound number, modulus of elasticity and flexure-toughness. Their performance was further investigated with respect to capillary surface rate of water absorption and accelerated corrosion testing involving impressed current initiated corrosion of concrete embedded reinforcement. Moreover, all test results were compared with a reference concrete cast without fibers.

4.1. Materials

4.1.1. Cement

Concretes are produced with a TS EN 197-1 CEM I (PÇ 42.5) Rapid Portland cement. Data showing the physical and chemical properties were reported by the material supplier and they are given in Table 4.1 and Table 4.2.

Table 4.1. Oxide and mineralogical components of cement (% by weight)

Oxide or Phase	Content, percent
SiO_2	20,80
Al_2O_3	4,90
Fe_2O_3	3,50
CaO	63,56
MgO	1,40
SO_3	2,63
Chloride Cl^-	0,0412
Na_2O/K_2O	0,18 – 0,85
C_3S	50,26
C_2S	21,80
C_3A	7,07
C_4AF	10,65
Insoluble Residue	0,80
Loss of Ignition	1,38

Table 4.2. Physical Characteristics of Cement

Specific Gravity (g/cm^3)	3,15	
Vicat	Start (min.)	144
	Stop (min.)	202
Specific Surface Area (cm^2/g)	3840	

4.1.2. Fibers

The physical characteristics of the fibers used are presented in Table 4.3. Pictures of the fibers are also presented in Figure 4.1. Hooked end steel fibers were used, provided adhered together in sets of tens with a water soluble adhesive according to ASTM A820. The polypropylene fibers used were fibrillated multi-filament fibers. The glass fibers were alkali resistant (AR) multifilament glass fibers, composed by 100 filaments each.

Fibers were incorporated into the concrete mix at fixed volume fractions. Steel fibers were 0.5 percent, polypropylene fibers were 0.1 percent and glass fibers were 0.1 percent by volume of concrete. Further properties of the used fibers, as reported by the supplier, are presented in Table 4.3.

Table 4.3. Physical Characteristics of the fibers used

	Steel	PP	Glass
Length (mm)	35	13	12
D (mm)	0,55	0,022	0,014
Length/diameter	64	591	857
Density g/cm^3	7,85	0,91	2,68
Tensile strength (MPa)	1100	400	1700
Mod. of Elasticity (GPa)	200	3,5-3,9	72
Fiber number/kg	14500	224 million	2,1 million

Figure 4.1. (a) Steel fibers, (b) Glass fibers and (c) Polypropylene fibers

4.1.3. Aggregates

The aggregates used are crushed sand, natural sand, and two different sizes of coarse aggregates. The physical characteristics of the aggregates used, as reported by the supplier, are given in Table 4.4. Aggregate sieve analysis was performed and results are presented in Table 4.5.

Table 4.4. Aggregate Physical Characteristics

	Unit weight (g/cm3)	Water Absorption (%)
Coarse Aggregate No 1	2,7	0,8
Coarse Aggregate No 2	2,74	1
Natural Sand	2,6	3
Crushed Sand	2,69	4

Table 4.5. Aggregate Sieve Analysis

Sieve size (mm)	31.5	16	8	4	2	1	0.5	0.25
Sieving Materials (%)								
No1	100	100	55	14	7	5	3	2
No2	100	60	3	0	0	0	0	0
Natural Sand	100	100	100	100	100	99	27	1
Crushed Sand	100	100	100	97	59	35	21	13

4.1.4. Superplasticizer

ASTM C 494 Type F high range water-reducing superplasticizer was utilized into the mixes in order to maintain approximately the same slump (17±2 cm). It is a Poly Naphthaline Sulphonate Condensate superplasticizer; the properties of the superplasticizer used are given in Table 4.6.

Table 4.6. Properties of Superplasticizer

Color	Dark Brown
State	Liquid
Specific Gravity, kg/l	1.2 ± 0.03
pH	6.50 – 8.00
Chloride Content	≤ % 0.1 (TS EN 480–10)
Alkali Content	≤ % 10 (TS EN 480–12)

4.2. Concrete Mix Properties and Concrete Casting

4.2.1. Concrete Mix Proportions

All concretes produced were cast using TS EN 197-1 CEM I Portland cement, crushed sand and natural sand as fine aggregates as well as coarse aggregate no.1 and coarse aggregate no.2 (as described in 4.1.3), water, superplasticizer and steel, polypropylene or glass fibers. All specimens prepared had 0,45 w/c. The mixture proportioning is tabulated in Table 4.7.

Table 4.7. Mixture proportioning (kg/m^3)

	Control	SFRC	PFRC	GFRC
Cement	400	400	400	400
Water	180	180	180	180
Course Aggregate No 1	575	575	575	575
Course Aggregate No 2	468	468	468	468
Sand	554	554	554	554
Fine Aggregate	235	235	235	235
SP	7	9	9	10.2
Steel fibers	--	39,25	--	--
PP fibers	--	--	0,91	--
Glass fibers	--	--	--	2,68

4.2.2. Concrete Casting

Concrete mixing was made in a laboratory mixer. The mixing sequence consisted of dry mix of the aggregates with cement. Then the cement was incorporated to the mix and mixed with water. Fibers were added and mixed before finally, water and superplasticizer were gradually added. Compaction was performed by rodding, vibration and tampering depending on the sample and the standards followed.

4.2.3. Concrete Test Specimens and Curing Conditions

A total of 16 100x200 mm concrete cylinder specimens were cast for the sorptivity test. These include 4 specimens with each fiber type and 4 control specimens with no fibers. For every group of 4 specimens two are wet cured for 28 days placed in a water tank at 20±2 and two are cured without any control in laboratory ambient conditions.

Similarly, another 16 100x200mm concrete cylinders were cast for the accelerated corrosion test, with the only difference that this time a 16mm diameter, 210 mm long steel rebar was placed in the centre of the mould. These specimens were cured without any control in laboratory ambient conditions.

A series of concrete specimens was produced with no fibers for reference and comparison, accompanying each fiber-reinforced concrete mix cast for each different test and curing regime.

4.2.4. Designation of tested Specimens

Further, for ease of expression and organization the following designation codes are used. The first letter designates the fiber used. *S* for steel fiber, *G* for glass fiber, *P* for polypropylene fiber and *K* stands for control, or for no fiber. The number *45* indicates the 0.45 w/c ratio. The following letter indicates the curing condition of the specimen; *C* for specimens that have been cured in the water tank and *N* for the specimens that have not been water cured. Finally the last number is either *1* or *2* indicating the two different specimens cast per cause. Designation of test specimens is presented in Table 4.8.

Table 4.8. Specimen code designation

Fiber Reinforcement	**w/c**	Curing Condition	Specimen No.	**Designation**
Steel	0.45	Cured	1	**S45C1**
Steel	0.45	Cured	2	**S45C2**
Glass	0.45	Cured	1	**G45C1**
Glass	0.45	Cured	2	**G45C2**
Polypropylene	0.45	Cured	1	**P45C1**
Polypropylene	0.45	Cured	2	**P45C2**
No fiber	0.45	Cured	1	**K45C1**
No fiber	0.45	Cured	2	**K45C2**
Steel	0.45	Non-Cured	1	**S45N1**
Steel	0.45	Non-Cured	2	**S45N2**
Glass	0.45	Non-Cured	1	**G45N1**
Glass	0.45	Non-Cured	2	**G45N2**
Polypropylene	0.45	Non-Cured	1	**P45N1**
Polypropylene	0.45	Non-Cured	2	**P45N2**
No fiber	0.45	Non-Cured	1	**K45N1**
No fiber	0.45	Non-Cured	2	**K45N2**

4.3 Test Procedures

4.3.1. Fresh concrete Properties

The freshly mixed concretes were tested for air content (ASTM C 231, pressured method), cone slump (ASTM C 143M-08) and density (unit weight) according to ASTM C 138M-08.

4.3.2. Mechanical Properties of Hardened Concrete

The mechanical properties that are tested in this study together with the methods used are listed below.

4.3.2.1. Compressive Strength. Compressive strength tests were performed on 100x200 mm cylinders of three companion specimens at the age of 28 days. The procedure followed during the test was in conformity with ASTM C39.

4.3.2.2. Split – Tensile Strength. Splitting tensile strength was derived by means of testing on 100x200 mm cylinder specimens as described in ASTM C496.

4.3.2.3. Static Elastic Modulus. To prevent stress concentration during the test, the specimens were capped prior to testing with a sulphur mortar in accordance with the specifications of ASTM C617. The test was conducted according to ASTM C469 at the age of 28 days.

4.3.2.4. Surface Hardness. The rebound number of hardened concrete surface for each mix was determined in accordance with the specification of ASTM C805 by using the specimens used in compression strength test.

4.3.2.5. Flexural Strength and Flexural Toughness. The flexural strength of concrete was obtained by testing 100x100x500 mm size test specimens under three-point loading. All the flexural tests were conducted on a 100 kN INSTRON close loop electric Universal Testing Machine. The specimens were turned on their side with respect to the position as cast before placing these on the support system so as to have a plain and uniform surface in contact with the supporting and loading rollers. The specimens were measured to determine their actual dimensions. Mid points and the location of the supports were marked in order to assure proper placement of the instrumentation. The beam was first placed on top of the support rollers. An LVDT for strain measurements was set at one side of the specimen at mid-span, to measure the mid span deflections. The test setup is shown in the Figure 4.2.

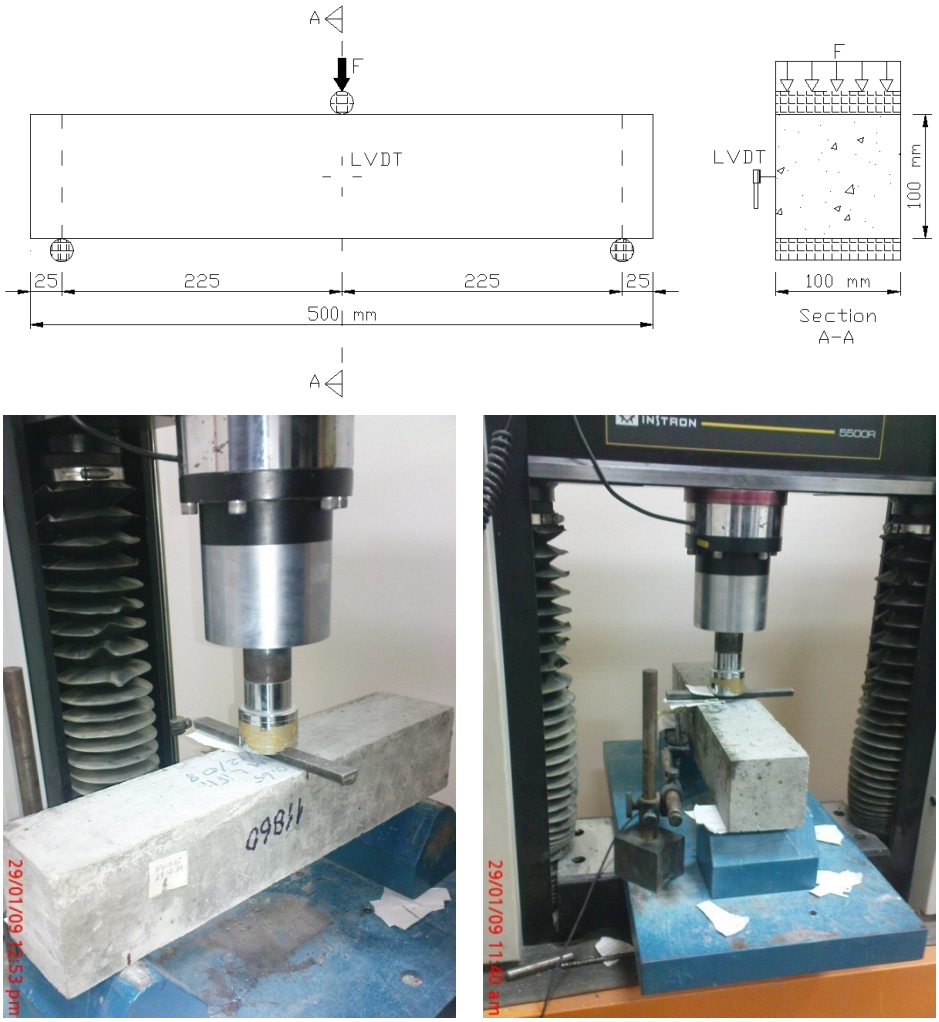

Figure 4.2. Flexure Test (top) Specimen dimensions, arrangement of the displacement transducers and loading conditions, (bottom) photo of the actual test setup with configuration of supports, loading and LVDT

The load was applied by the INSTRON Universal Testing Machine through the head of the machine to the top face of the specimen at mid-span. A thin steel plate is positioned between the loading head and the specimen to distribute the load over the specimen width. The head of the machine was initially lowered so that it was touching but not loading the top steel plate. Measurements were recorded by a data-acquisition system.

The load application was deflection controlled at a rate of $0.3 * 10^{-3}$ mm/min. The complete load deflection curve was obtained for each specimen tested. The first crack load, defined as the point at which the load deflection curve first deviates from linearity and the maximum load attained was noted for each test specimen.

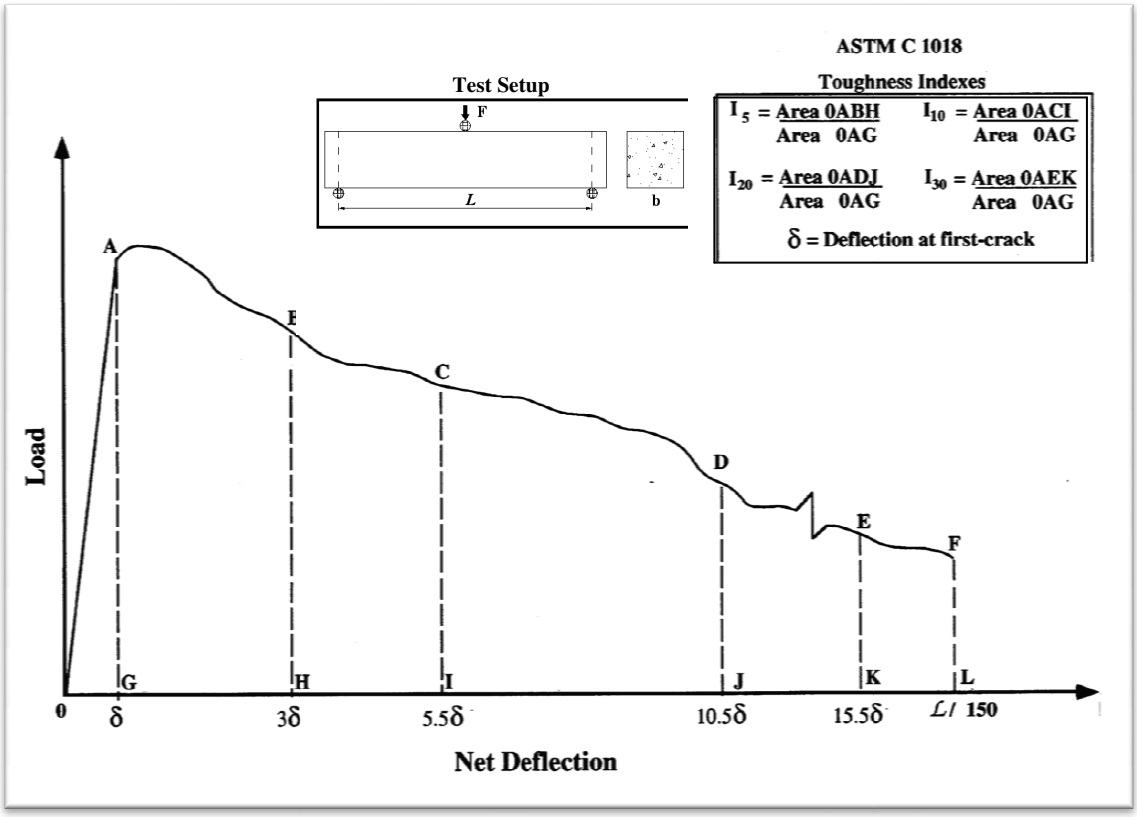

Figure 4.3. Techniques of Fiber Reinforced Toughness Characterization [27]

The flexural toughness was obtained from the results of the same flexure test, described above. Toughness indices I_5, I_{10}, I_{20}, I_{30}, etc., are calculated by taking the ratios of the energy absorbed to a certain multiple of first crack deflection and the energy consumed up to the occurrence of first crack (Eqn. 4.1). A three point loading test is performed in this study whereas in ASTM C 1018 results from a four point loading test are used. A description of the use of the toughness indices is given in Figure 4.3. Generally,

$$I_N = \frac{Energy\ absorbed\ up\ to\ a\ certain\ multiple\ of\ first\ crack\ deflection}{Energy\ ansorbed\ up\ to\ the\ first\ crack} \tag{4.1}$$

where subscripts N in the I_N indices are based on the elastic-plastic analogy such that, for a perfectly elastic-plastic material, the index I_N would have a value equal to N. The scheme compares a given FRC with a conceptual material that behaves in an ideally elastic-plastic manner. Implicitly, the scheme also assumes that plain concrete is ideally brittle and, hence, the various toughness indexes for plain concrete are assumed to be of a constant value of one [27].

4.3.3. Sorptivity Test

This test method is used to determine the rate of absorption (sorptivity) of water by concrete and fiber reinforced concrete, by measuring the increase in the mass of a specimen resulting from absorption of water as a function of time. Only one surface of the specimen is exposed to water at room temperature while the other surfaces are sealed. The exposed surface is immersed in water and water ingress of unsaturated concrete is then dominated by capillary suction during contact with water. This method is intended to determine the susceptibility of an unsaturated concrete to the penetration of water.

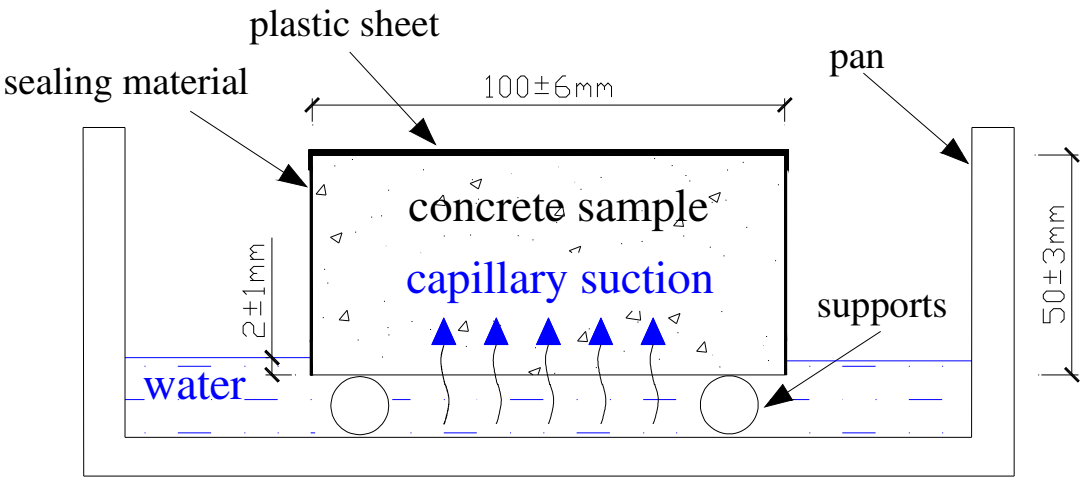

Figure 4.4. Sorptivity Test Configuration

The sorptivity test was carried out according to the ASTM Designation C 1585-04. The apparatus used and the test setup are presented in Figure 4.4. Low permeability epoxy paint was carefully brushed on the side surfaces to act like sealing material and a plastic sheet was placed on the top and sealed with an elastic band in order to control evaporation. Specimens are obtained from cylinders molded according to practice C 192/C 192M. Two specimens are tested for each concrete type and curing condition.

Sample conditioning and weighing prior to testing was performed in accordance with ASTM C 1585-04. The specimens are placed on two supports in pans containing water and at the same time the stop watch is started. The concrete specimen masses are

weighed at specific time intervals. The water is kept at a constant level by refilling to the measured point daily.

Sorptivity coefficients for initial absorption and secondary absorption are calculated for all specimens by the method described in ASTM C 1585 - 04. Measured values of mass at specific time intervals during the experiment, together with the specimen dimensions, allow for absorption, *I*, to be calculated for each time interval (see Eqn. 4.2).

$$I_{abs} = \frac{m_t}{A_{exp}/d} \tag{4.2}$$

where I_{aps} is the absorption, m_t is the change in specimen mass (grams), at the time t (seconds), A_{exp} is the exposed area of the specimen (mm^2) and d is the density of water (g/mm^3).

Absorption values (mm) are then plotted against the square root of time ($sec^{1/2}$). The initial rate of water absorption or initial sorptivity coefficient is obtained by using least-squares, linear regression analysis of the plot of *I* versus $time^{1/2}$, for points from one minute to six hours. The secondary rate of absorption is obtained by the same way but for the points from one day to seven days. However the results within these two ranges should follow a linear relationship with a minimum correlation coefficient of 0.98, otherwise the rate of absorption cannot be determined. Also in case the last values considered in deriving the initial rate of absorption show a clear deviation from the linear relationship developed, they should be excluded.

4.3.4. Accelerated Corrosion

An accelerated corrosion technique is used by means of an impressed current, anodically polarizing the concrete reinforcement. The specimen is supported upwards in an alkaline solution whose water level reaches approximately the top surface of the specimen. A cylindrical stainless steel sheet is positioned concentrically surrounding the specimen. A constant voltage of 30 V is applied from the external *DC* source between anode and

cathode. The electrolyte is 70 gram per liter sodium chloride (*NaCl*) water solution. The setup of the experiment is presented in Figure 4.5.

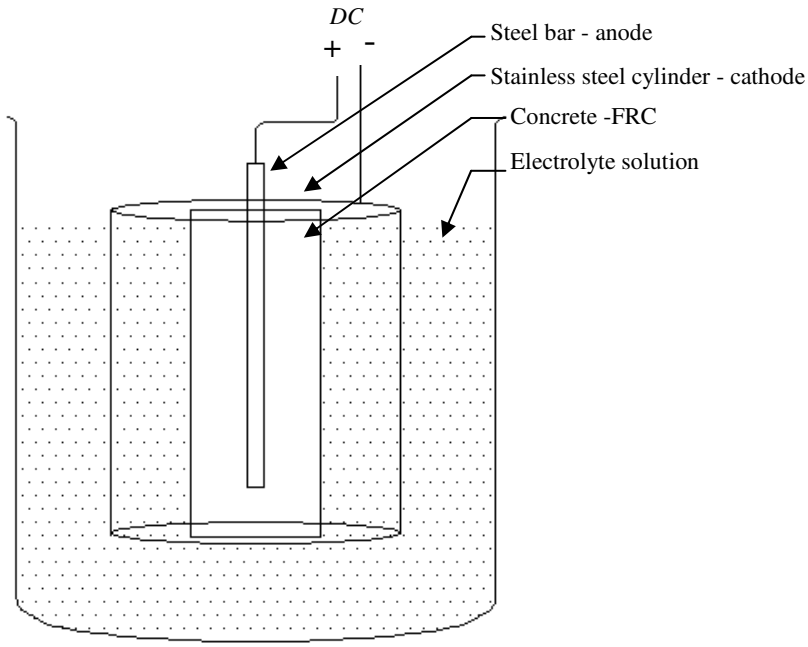

Figure 4.5. Schematic of Accelerated Corrosion Test Setup

The embedded rod acts as an anode and the cylindrical stainless steel acts as a cathode forming a closed electrical circuit, within which the concrete cover and the electrolyte solution separate the two poles and together act as the circuit resistance. A reference resistance (R_1) of 11 Ohm is added to the circuit. The value of the current (V_1) of the reference resistance is continuously observed through a software (TDG CODA Locomotive) and measurements are saved every one minute by the data logger.

As already mentioned, a 30 Volt potential is constantly applied to the electrical circuit and voltage measurements going through the reference resistance are taken every minute and saved to the data logger, to be able to observe the stages of corrosion. The test setup is presented in Figure 4.6 as an electrical circuit.

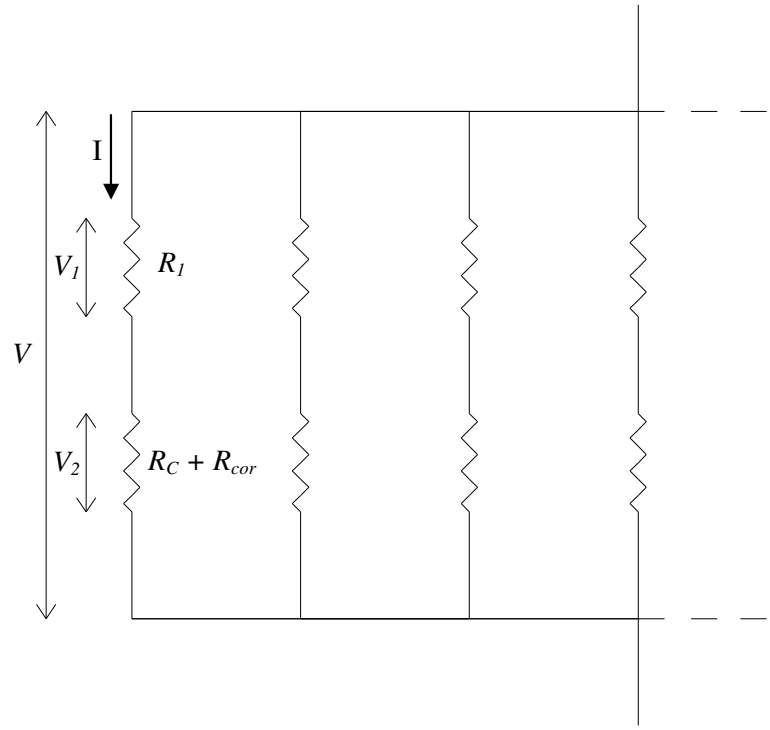

Figure 4.6. Accelerated corrosion test setup as electrical circuit

By incorporating Ohm's Law (Eqn. 3.8) the variation of the current and resistances in the circuit will be determined. Using the measured volt value (V_1) and the known resistance R_1, the current (I) passing through can be calculated (Eqn 4.3). The first value of I, at the beginning of the test, and Equation 4.4 can be used to calculate the initial cover resistance R_C (Eqn. 4.5).

$$I = V_1/R_1 \tag{4.3}$$

$$V = I(R_1 + R_C) \tag{4.4}$$

$$R_C = R_1\left(V/V_1 - 1\right) \tag{4.5}$$

At this time and up to the first crack the observed R_C is assumed to remain constant and the decrease of the current passing through the circuit is attributed to the initiation of corrosion. At the first crack point the potential difference measured at the reference

resistance (V_2) will provide the necessary information upon calculating the current passing through the circuit at cracking point I_2 (Eqn. 4.6).

$$I_2 = V_2/R_1 \tag{4.6}$$

Corrosion formed around the steel bar increases the total circuit resistance continuously up to cracking of concrete cover. The maximum resistance increase caused by corrosion of the steel bar R_{cor} can be determined with Equations 4.7 and 4.8:

$$V = I_2(R_1 + R_C + R_{cor}) \tag{4.7}$$

$$R_{cor} = \frac{VR_1}{V_2} - R_1 - R_C \tag{4.8}$$

The time to initiate a first crack on the concrete is also observed along with the corresponding anodic current. At the time of first crack a specimen is removed in purpose of determining the amount steel bar mass loss due to corrosion needed to initiate concrete cover cracking.

Further, the post crack behavior of the different specimens is observed visually and by means of current measurements variation over elapsed time. The effect of the different fibers in crack propagation can be compared with observations during the crack propagation phase of this test. The total charge can be calculated from the area of the current-time curve.

5. TEST RESULTS AND DISCUSSION

5.1. Fresh Concrete Properties

All concrete mixes were cast with a slump of 17 ± 2 cm. This was achieved by using a high range water-reducing admixture at the required dosage as reported above in Table 4.7. Therefore slump was performed in order to assure the desired quality of concrete was achieved. Table 5.1 presents the fresh concrete properties obtained. Apart from the fiber addition, all other concrete components are of the same type and the casting and compacting methods are the same for FRC and control concrete. It is obvious that control concrete has less air content than the FRCs.

Table 5.1. Fresh Concrete Properties

	Control	**SFRC**	**PFRC**	**GFRC**
Slump (cm)	18.7	15.8	16.6	17.1
Density (gram/dm^3)	2333	2345	2320	2306
Air Content (%)	1.3	3.4	3.7	4.8

Further it is noted that no steel fibers are visible on SFRC specimen surfaces whereas glass and polypropylene fibers are visible on the specimen surface. Steel fibers and fibrillated polypropylene fibers have low water absorption in contrast to high water absorption glass fibers.

5.2. Mechanical Properties

5.2.1. Compressive Strength

A summary of test results of the compressive strength of all the concretes is presented in Table 5.2.

Table 5.2. Compressive Strength (MPa)

Test Specimen	Average Compressive Strength (MPa)
Control	48.5
SFRC	55.6
PFRC	55.5
GFRC	47.2

SFRC and PFRC have the highest compressive strength in comparison to GFRC, exhibiting a 15 percent increase of compressive strength in comparison to control concrete. But GFRC did not produce a higher compressive strength than control concrete. In contrast to the other FRC tested, GFRC compressive strength was 3 percent lower than control concrete.

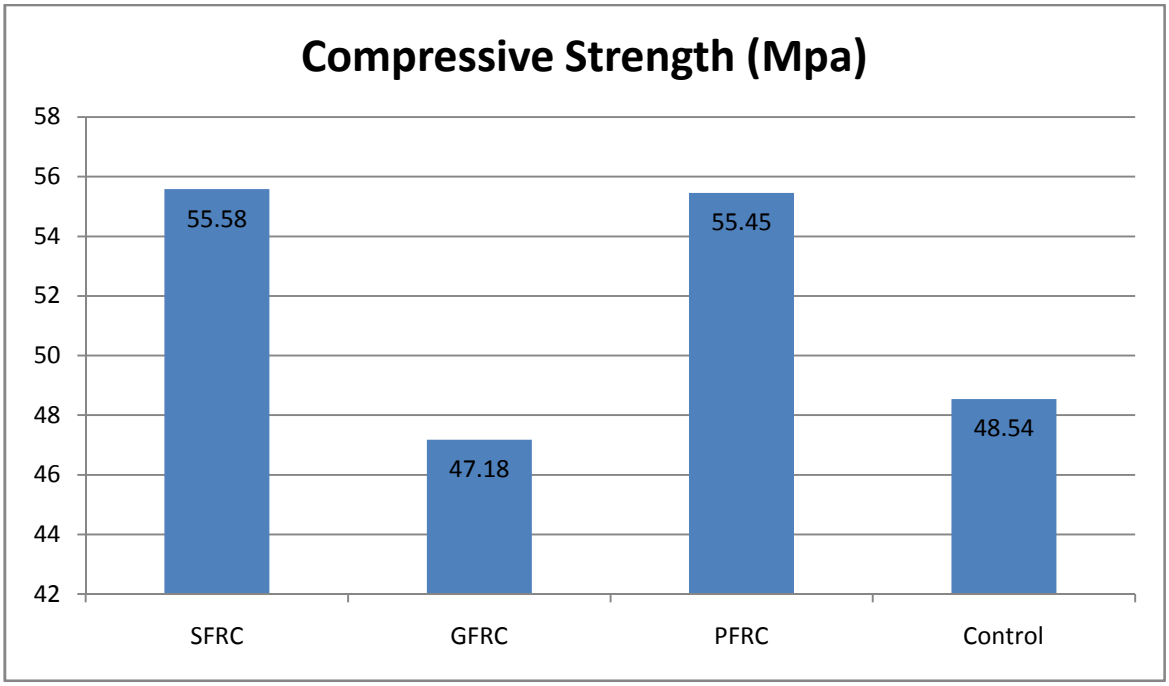

Figure 5.1. Compressive Strength (MPa)

The effect of fiber addition to FRC compressive strengths obtained in previous research is not so clear. SFRC compressive strength was not significantly increased in [9, 12], which does not comply with the increase observed in the current research. Polypropylene fibers are not reported to significantly alter the compressive strength of concrete [17], however, according to [3] polypropylene fiber volumes of at least 0.2 percent should enhance compressive strength. The PFRC compressive strength obtained herein is considered to be significantly higher than plain concrete compressive strength. The compressive strength of GFRC is found to be similar to control concrete but slightly decreased. This result agrees with previous research [16, 20].

5.2.2. Splitting Tensile Strength

The splitting tensile test results obtained as maximum attained load were used in Equation 5.1 below to derive tensile strengths. The results are given in Table 5.3 and Figure 5.2.

$$f_t = \frac{2P}{\pi D L}; \quad (5.1)$$

where f_t is the tensile strength in MPa; P is the maximum applied load indicated by the testing machine in N; D and L are the cylinder diameter and length, respectively in mm.

Table 5.3. Tensile Strength (MPa)

Test Specimen	Average Tensile Strength (MPa)
Control	3.4
SFRC	4.1
PFRC	2.9
GFRC	4.0

Steel fiber-reinforced concrete has produced the highest values of tensile strength. In comparison to control concrete tensile stress is on average increased by 20 percent by steel fiber addition. However, considering the range of the results obtained, a maximum observed increase in SFRC tensile strength was 60 percent. These results comply with previous research results. In [12] tensile stress of 0.45 w/c SFRC, with the same mixture and fiber properties as the ones considered in this research, is reported to be on average 25 percent higher than control concrete tensile stress. GFRC behaved almost the same with SFRC achieving on average high tensile strengths. PFRC on the other side has a lower tensile strength than control concrete. A 15 percent decrease in tensile strength is observed by addition of polypropylene fibers. This PFRC behavior has also been reported in previous studies [1].

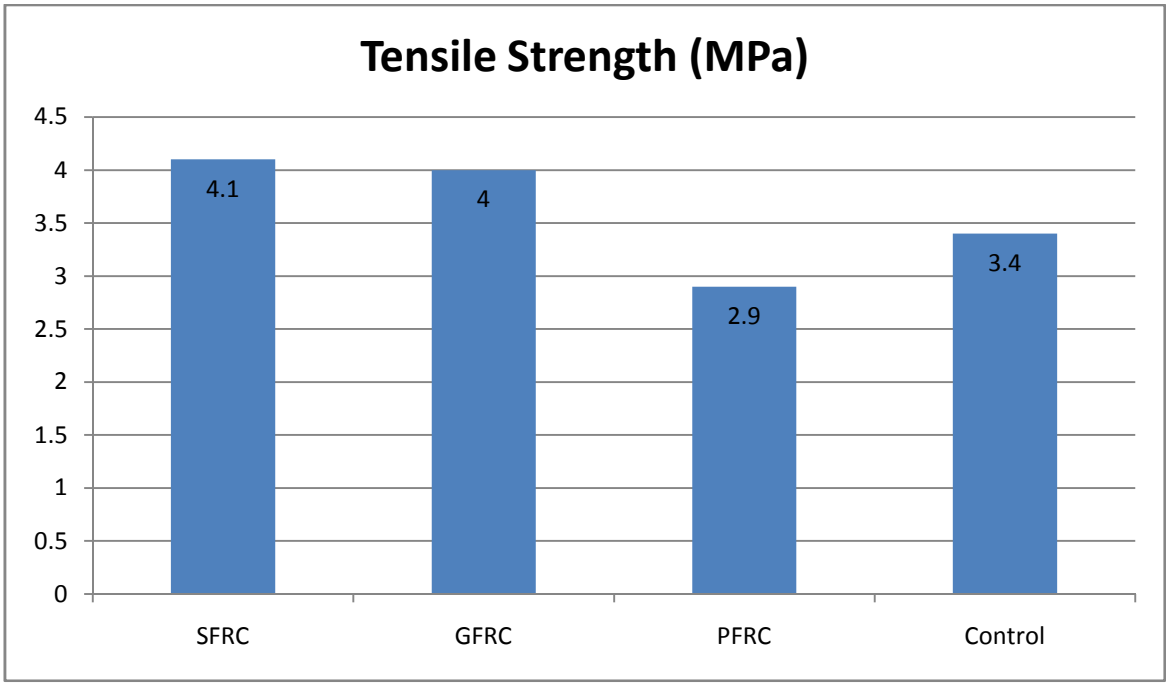

Figure 5.2. Tensile Strength

5.2.3. Modulus of Elasticity

The Modulus of Elasticity was obtained according to ASTM C469-02. The results obtained are presented in Figure 5.3 below.

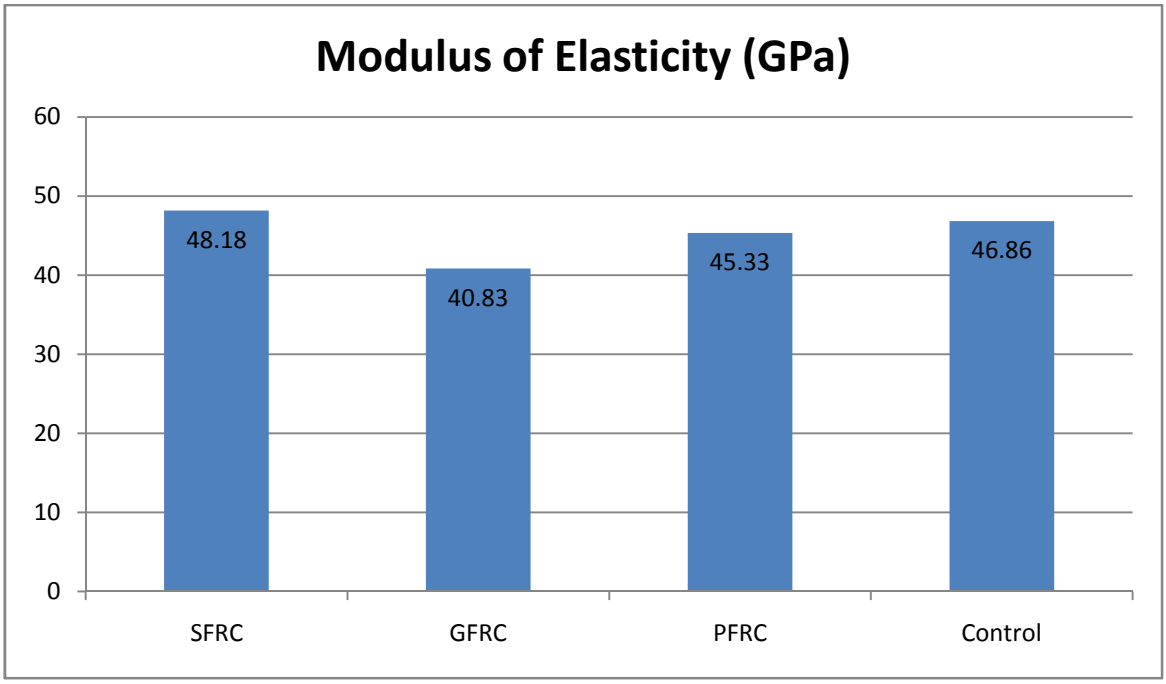

Figure 5.3. Modulus of Elasticity

In general the SFRC and PFRC modulus of elasticity are not significantly different to plain concrete modulus of elasticity. Results of previous research on FRC properties have not reached a clear outcome upon the effect of fibers on concrete modulus of elasticity but in general for fiber volume percentages similar to fiber volume percentages used in this study no significant change is expected. However, it should be noted that GFRC in this report has a decreased (13 percent lower) modulus of elasticity in comparison to control concrete.

5.2.4. Rebound Number

The surface hardness of the concretes was measured by means of the Schmidt hammer, prior to the compression test. The averages of ten rebound numbers yielded for each FRC are presented in Figure 5.4 and in Table 5.4 together with compressive strength values obtained.

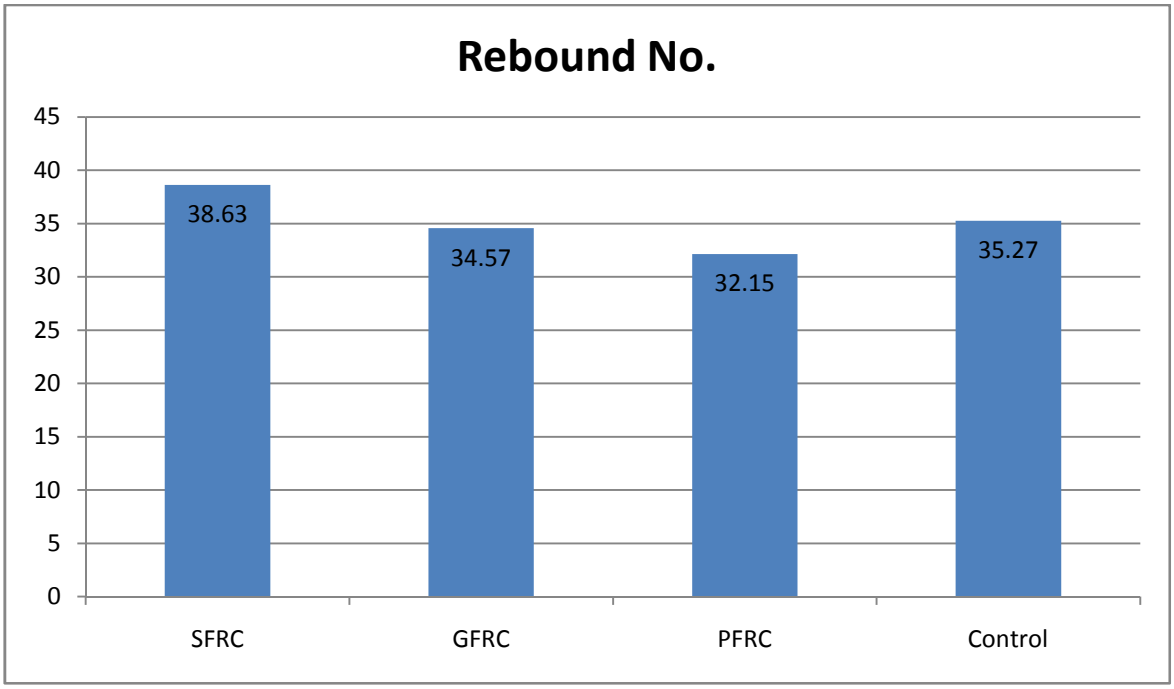

Figure 5.4. Rebound Number

Table 5.4. Rebound number and Compressive Strength

Specimen	Rebound No.	Compressive Strength (MPa)
Control	35.3	48.5
SFRC	38.6	55.6
PFRC	32.2	55.5
GFRC	34.6	47.2

SFRC rebound numbers obtained are on average 10 percent higher than control concrete rebound numbers. PFRC values of rebound numbers are on average 8 percent lower than control concrete. GFRC rebound numbers are slightly (2 percent) lower than those obtained for control concrete. The rebound numbers obtained for the FRC in correlation to the compressive strengths obtained appear to generally agree. SFRC and PFRC compressive strengths were both higher than control concrete by about 15 percent. GFRC compressive strength was 3 percent lower than control concrete.

5.2.5. Load-Deflection Curves and Toughness

The flexural test results are presented in Figures 5.5-5.7 and Table 5.5. The flexural strength is determined from the maximum load reading in accordance with ASTM C 78. SFRC and GFRC on average withstand a 5 and 7 percent higher maximum load respectively, than control concrete. PFRC, on the other hand, withstands a maximum load of 8269 N which is 5 percent lower than control concrete. FRC flexural stresses percent deviation from control flexural stress are the same as for maximum load, as the specimen dimensions and loading setup are the same.

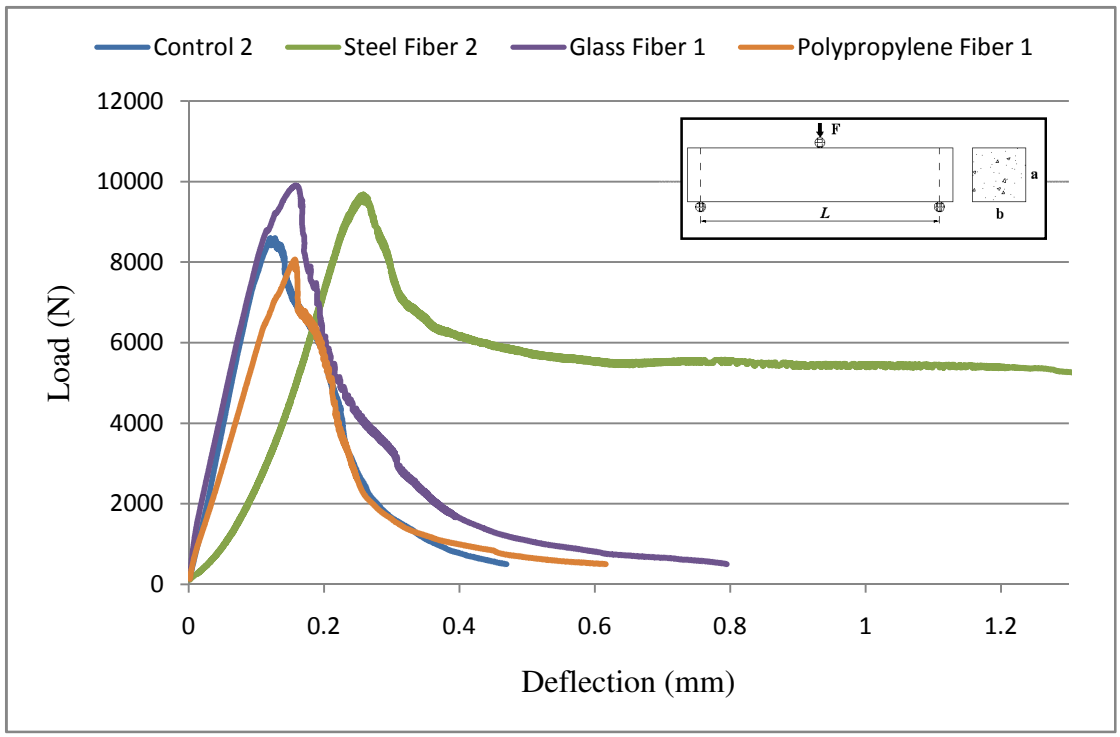

Figure 5.5. Flexural Load-Deformation graph for SFRC, GFRC, PFRC and control concrete

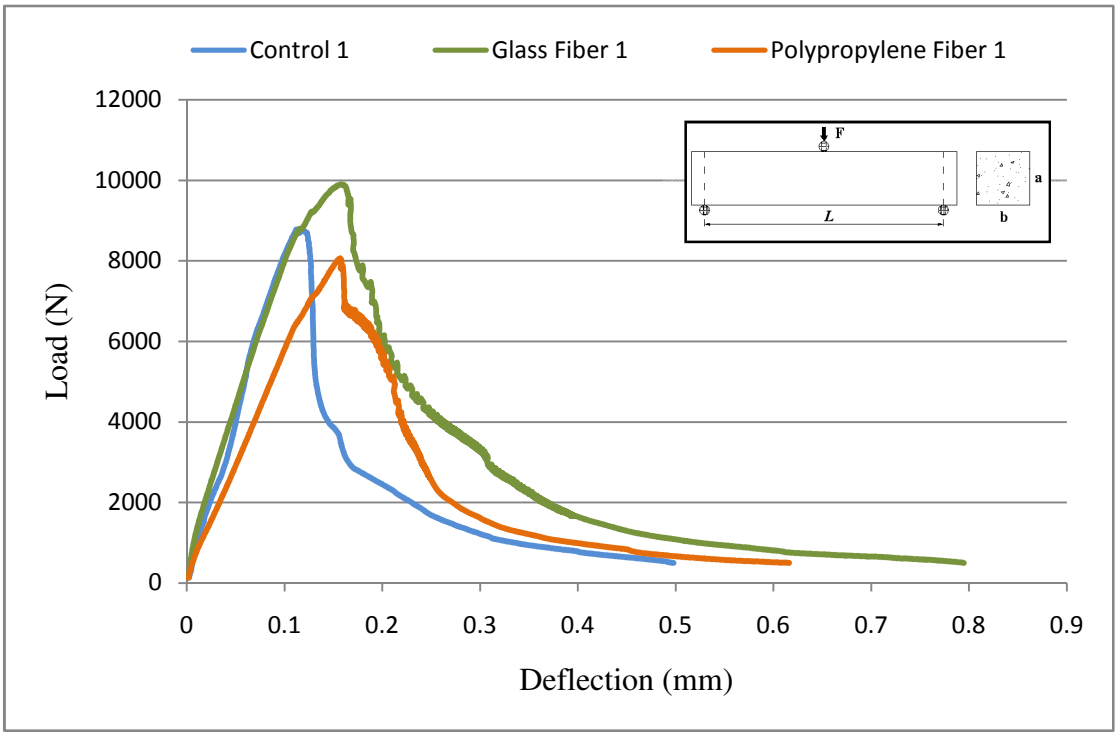

Figure 5.6. Flexural Load-Deformation graph for GFRC, PFRC and control concrete

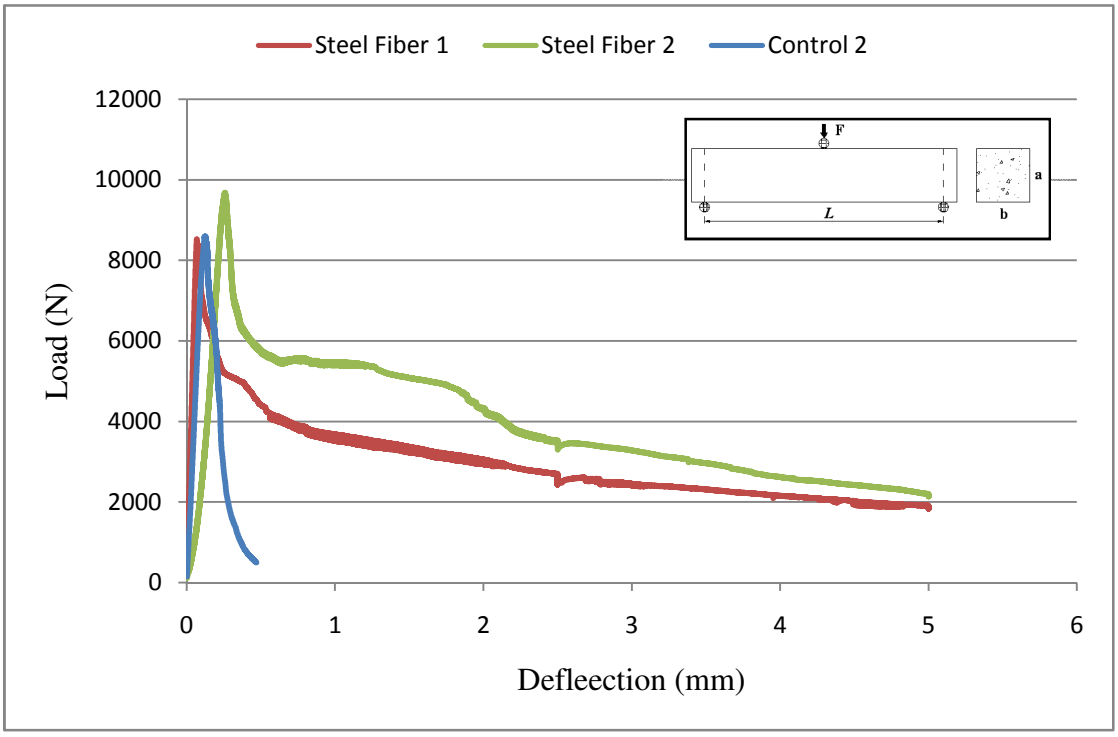

Figure 5.7. Flexural Load-Deformation graph for SFRC and control concrete

Table 5.5. Flexure - Toughness Test Results

	SFRC	GFRC	PFRC	Control
Fracture Energy, G_f(kg/sec2)	*1778.2*	*219.2*	*172.3*	*147.3*
Flexural Stress (Mpa)	*5.46*	*5.56*	*4.96*	*5.21*
Maximum Load, P_{max} (N)	*9107*	*9263*	*8269*	*8688*
Deflection at P_{max} (mm)	*0.163*	*0.199*	*0.112*	*0.116*
Maximum Deflection (mm)	*5.00*	*0.68*	*0.69*	*0.48*
Toughness Index I_5	*3.69*	*2.14*	*2.58*	---
Toughness Index I_t	*11.94*	*1.46*	*1.14*	---

From Figure 5.6 it can be observed that FRC attain a maximum load at a point past first crack. Initially, the deflection increased linearly as the load was increased up to a strength where the members' elastic limit is reached. At this point the matrix first crack is initiated. On the curves the matrix first crack, or elastic limit, can be observed as the first point of deviation from linearity. FRC possess considerable load and strain capacity beyond the matrix cracking strength.

The energy absorbed by the specimen is represented by the area under the complete load-deflection (*P-d*) curve. In order to compare the toughness of the tested specimens the toughness index I_5 is determined as recommended by ASTM C 1018, taking under consideration the ratio of the area of the load-deflection curve up to three times the deflection attained at maximum load over the area under the curve up to the point of maximum load. This index provides an indication of the relative toughness of the tested FRC at these deflections. The toughness index I_t is a measure of the improvement in toughness relative to the unreinforced matrix, considering the ratio of the total area under the FRC *P-d* curve over the total area under the control concrete *P-d* curve.

The fracture energies are determined, as the potential energy and the total area under the load-deflection curve over the specimen cross-sectional area. The fracture energies (G_f) obtained indicate the higher toughness of FRC in comparison to plain concrete. SFRC exhibited exceptionally high fracture energy. In Figure 5.5 it can be observed that the post cracking behavior of SFRC is significantly enhanced in comparison to the other FRC and the control specimen. The G_f of SFRC being 1778.2 kg/sec^2 is over 12 times higher than control concrete. GFRC also produced significantly increased fracture energy, on average 50 percent higher than control concrete. PFRC G_f values are on average 17 percent higher than control concrete.

The flexure-toughness results obtained for the FRC tested in this study generally appear to comply with previous research. SFRC is obviously advantageous in terms of toughness because of its post cracking behavior. The hooked end fibers added to concrete formed mechanical anchors in concrete, bridging the forming cracks which resulted in higher loads retained at larger deflections. It was the only sample that did not suddenly break into two separate pieces during the flexural test but it retained its structural integrity while multiple cracks were gradually developed with increasing deflection, by distributing stress to the broader region. This observation was also reported in [9].

GFRC results comply with previous reports [11, 31]. Similar ultimate flexural strength increase due to glass fibers was obtained in [16] and in [20].

PFRC has produced a lower flexural stress (5 percent) than control concrete reaching ultimate load at a slightly smaller deflection (3 percent), therefore disagreeing with the improved flexural characteristics reported in [11]. However, PFRC produced improved toughness characteristics withstanding a 43 percent higher maximum deflection than control concrete; results complying with those in [17].

5.3. Sorptivity Coefficient

The results obtained from the sorptivity test are presented in Table 5.6, Table 5.7 and in Appendix B. A comparison of the sorptivity coefficients of the different fiber-reinforced concrete specimens depending on the fiber type and the different curing regimes they were succumbed to is presented below.

Table 5.6. Initial Sorptivity Coefficients

Specimen	Initial Sorptivity Coefficients ($cm/s^{1/2}$)
K45C	0.00359
K45N	0.00528
S45C	0.00315
S45N	0.00410
G45C	0.00358
G45N	0.00493
P45C	0.00329
P45N	0.00471

Table 5.7. R-squared of Initial Sorptivity trend line

	C1	C2	N1	N2
SFRC	0.9908	0.9824	0.9943	0.9937
GFRC	0.9867	0.9842	0.9902	0.9943
PFRC	0.9920	0.9915	0.9970	0.9965
Control	0.9913	0.9820	**0.9412**	0.9878

It is clearly observed that fiber addition appears to reduce the rate of water absorption of concrete, as the unreinforced 'control' specimens produce the highest sorptivity coefficient values. It should be noted that the initial absorption rate results obtained for control concrete are comparable to results obtained in previous researches.

Steel fibers have reduced the sorptivity the most, in comparison to the polypropylene fibers and glass fibers. Cured SFRC initial absorption rates were very similar for both test specimens and were 12 percent lower than control concrete. Non cured SFRC produce an initial absorption rate on average 26 percent lower than non cured control concrete, ranging from 24 to 29 percent lower.

Polypropylene fibers also reduced the rate of water absorption of concrete. P45C initial absorption rates on average 8.5 percent lower than K45C, ranging from 7 to 10 percent. P45N initial sorptivity coefficients are equal for both tested specimens and 15 percent lower than K45N.

Glass fibers produced the least reduction of initial sorptivity coefficients in comparison to the other fibers used. Cured GFRC produces a negligible 0.3 percent lower initial water absorption rate than control concrete. However, the two results obtained oppose each other, one showing about 9 percent reduction and the other an 8 percent increase in comparison to control concrete, do not allow a clear understanding of the cured GFRC initial water absorption behavior. The non cured GFRC produced, on average, 11 percent lower initial sorptivity coefficients than control concrete, ranging from an 9 to a 13.5 percent decrease.

Within all the specimens tested there was only one specimen, that of control K45N1, whose initial water absorption rate could not be derived because the data obtained did not follow a linear relationship. The correlation coefficient (R^2) of the slope of the line formed by the initial absorption values for K45N1 was 0.9412. It was observed that the rate of water absorption within the first five minutes of testing K45N1 was considerably high, causing a deviation from the later on linearly increasing values.

Similarly, the correlation coefficients of the linear regression analysis performed to find the line of best fit to the absorption values from one day to seven days, where unacceptably low in order to derive secondary rates of water absorption for all specimens. The order by which non cured specimens' R^2 results deviate from the acceptable limit of R^2= 0.98 is control concrete, SFRC, PFRC and the furthest GFRC with 2.6, 3.4, 5 and 6 percent deviation respectively. For cured specimens the R^2 results of control concrete, SFRC, PFRC and GFRC are 0.2, 3.7, 3.5 and 3.5 percent respectively. Therefore the secondary rate of water absorption is not considered for the tested specimens.

However, the total mass absorbed by FRC in the secondary phase can comparatively indicate the sorption behaviors at this phase. The total mass absorbed by each specimen from six hours until the end of testing is presented in Table 5.8.

Table 5.8. Total mass absorbed during secondary phase

Specimen Type	Average mass increase in secondary phase (grams)	
	Cured	Non-Cured
Control	7.58	9.95
SFRC	5.13	7.85
GFRC	5.39	8.72
PFRC	5.20	8.73

It is obtained that during the secondary phase FRC absorbs less water than plain concrete. Comparing to plain concrete results obtained for cured SFRC, GFRC and PFRC were 32, 29 and 31 percent, respectively, lower than cured plain concrete. For non-cured SFRC, GFRC and PFRC results were 21, 12 and 12 percent, respectively, lower than non-cured plain concrete. SFRC exhibited the less water absorptive behavior in comparison to PFRC and GFRC, whose behaviors were similar, for both curing conditions. As in the initial phase SFRC continued to absorb less water than PFRC and GFRC.

As derived, FRC air content is higher than plain concrete. The air content percentage within concretes is a parameter generally implying higher water penetrability because of the broader pore structure; thus, implying that the FRC water sorptivity should be greater than plain concrete. On contrast, FRC was proven to have lower rate of water absorption than plain concrete, therefore other effects of fibers on concrete water sorptivity are involved.

Also in comparison of the different FRC sorptivity coefficients derived and their air content percentage, it is understood that the expected air content-water absorption relationship applies between FRCs. SFRC has the least air content compared to the other FRC and exhibits the least water absorption. GFRC on the other hand has the highest air content and the highest rate of water absorption in comparison to SFRC and PFRC.

Correlation of the FRC sorptivity results is also observed with their compressive strengths obtained. In general, concrete with higher compressive strength have lower water absorption [40]. SFRC having the highest compressive strength between the FRC considered also exhibits the lowest water absorption. GFRC on the other hand has the lowest compressive strength and the highest water absorption between the FRCs. But in comparison to control concrete GFRC has a lower compressive strength and a reduced rate of water absorption, whereas SFRC and PFRC have higher compressive strength than control concrete and reduced rate of water absorption.

5.4. Accelerated Corrosion Test

5.4.1. Test Results

The current I_1 (First Current) passing through the considered FRC is derived by use of Equation 4.3 and the reading of the value of V_1 at the beginning of the test. The current passing through the test specimens decreases with time as the resistance of the corrosion formed around the steel bar increases. First, the current drop from initiation of the test up to its minimum value at the formation of the first cracks, and the time up to this point are

considered. Then the electrical charge Q, calculated as the area under the current-time curve, is considered . Results obtained are tabulated in Table 5.9.

Table 5.9. Accelerated Corrosion Results

	SFRC	GFRC	PFRC	Control
First Current (mA)	238	160	114	132
R_C (Ohm)	115.0	176.5	252.2	216.3
Average time to crack initiation (hours)	11.8	25.5	39.0	21.4
Current drop to crack initiation (mA)	125	65	57	65
R_{corr} (Ohm)	140.4	128.3	265.0	223.2
Initial mass loss (grams)	1.46	1.35	1.2	1.59
Q up to crack initiation (A.sec)	4.6	8.2	10.8	7.4
Current rise from crack initiation to 2 hours after (mA)	3.9	1.0	1.6	0.7
Q total (A.sec)	194.4	356.9	102.9	154.1

5.4.2. Test Initiation

The values of first current are determined for reference and use in further needed calculations. However, the first current passing through SFRC was clearly higher than the other tested specimens and does not satisfy correlations with other hardened concrete test results obtained. There is reason to believe that the steel fiber electrical resistivity allows higher current to pass through the SFRC cover. Therefore the results obtained for SFRC from the impressed voltage accelerated corrosion test are affected by a parameter which

further accelerates the test thus consisting them incomparable with the results for other FRC.

The initial concrete-cover resistance R_C is calculated by use of Equation 4.5. R_C is a value indicating the concrete cover electrical resistance. Results obtained show that the lowest R_C was exhibited by SFRC in comparison to the other tested specimens as it is 47 percent lower than control concrete R_C. PFRC R_C is 16 percent higher and GFRC R_C is 18 percent lower than control concrete R_C. The high electrical conductivity of SFRC cover causes an exceptional lower resistance to the current that goes through it, from the beginning of the test.

5.4.3. Crack Initiation

It is realized that the value of the first current going through each specimen is decisive for the time needed for the cover crack initiation. In comparison of the elapsed time up to the first crack and the first current read for each specimen it is observed that they are inversely proportional. SFRC with the highest first current reading and therefore the least cover concrete resistance withstands cracking for a shorter time than the other specimens that crack one at a time in an ascending order according to their initial resistances.

The current drop from initial to the lowest point, the time duration and the electrical charge (the area under the current-time curve) to the lowest current value, together with the values of the resistance caused by the corrosion product (R_{corr}) and the rebar mass loss at the point of first crack obtained for each specimen provide important information about FRC reinforcement corrosion induced crack initiation.

It can be observed that cracking in SFRC is formed first and together with the steepest and highest current drop it had the least charge passing through it because of the comparatively very small time duration up to cracking. PFRC withstood cracking for the longest time reaching 39 hours of exposure to electric potential before cracking. PFRC also experienced the least current drop before cracking and the highest electrical charge up to

crack initiation. The electrical charge needed to crack PFRC was 45 percent more than that needed to crack control concrete. GFRC electrical charge up to cover crack initiation was 10 percent more than the respective charge obtained for control concrete, because of the longer time elapsed up to cracking.

FRC tensile strengths obtained from the splitting tensile test are correlated to the steel bar mass loss at first crack and the time duration up to crack initiation. At the point of crack initiation and at the end of the corrosion phase, corroded reinforcing bars are removed and cleaned in hydrochloric acid according to the ASTM G1-03 standard, and weighed to get the actual degree of mass loss. Results obtained for the steel bar mass loss due to corrosion at initiation of cracking and at the end of the experiment are given in Table 5.10 together with the corresponding time elapsed until crack initiation and until each test was terminated. Also their corresponding tensile strengths are given in the same table, as obtained previously.

Table 5.10. Mass Loss at cracking point and Split Tensile Strength

	Mass Loss (grams)	Time (hours)	Average Tensile Strength (MPa)
Control	1.59	45.5	3.4
	37.03	146.5	
SFRC	1.46	24.0	4.1
	34.01	146.5	
PFRC	1.20	45.5	2.9
	19.00	146.5	
GFRC	1.35	26.5	4.0
	85.58	146.5	

SFRC having the highest tensile strength also withstands the most rebar mass loss prior to cracking in comparison with the other FRC test results. The corrosion products

formed in SFRC at first crack are eight percent lower than that needed to crack control concrete. SFRC fast corrosion attributed to the steel fiber conductivity provides an easy path to the current to induce corrosion but the corrosion products formed around the steel bar do not follow the same route towards the cathode. They are concentrated around the rebar and induce pressure to the SFRC cover as they develop, similarly for all specimens in this test. But the corrosion of the steel fibers is believed to introduce weak points through the concrete fibers and alter the fiber properties, therefore allowing the dispersion of the rebar corrosion products and finally allowing easier crack initiation.

Further, Figures 5.8 and 5.9 are given in order to observe the test specimens and the removed and cleaned steel bars at the time of cracking.

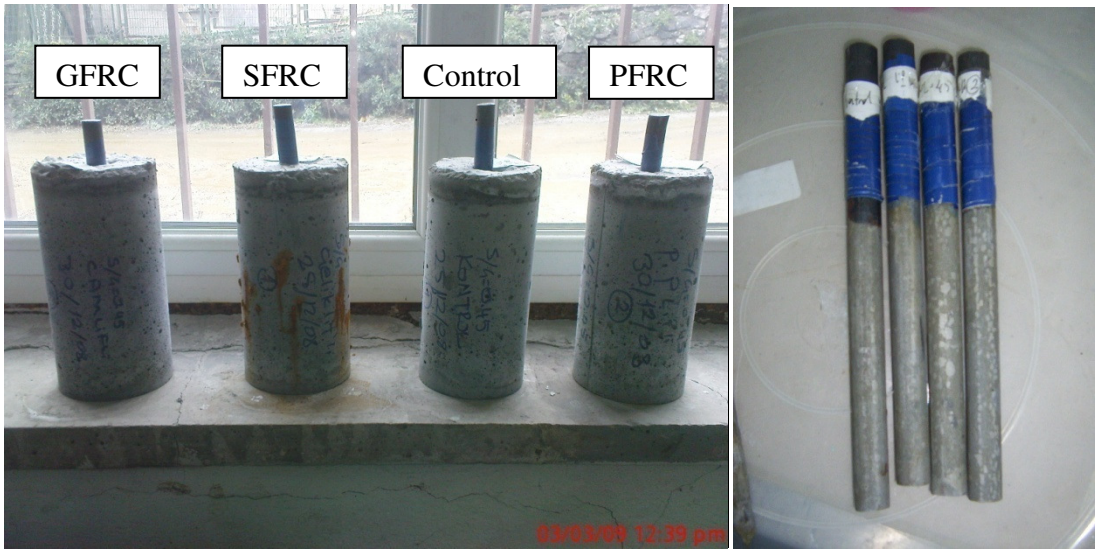

Figure 5.8. Specimens at first crack and steel bars after removing and cleaning (from left to right: removed from control concrete, SFRC, PFRC and GFRC)

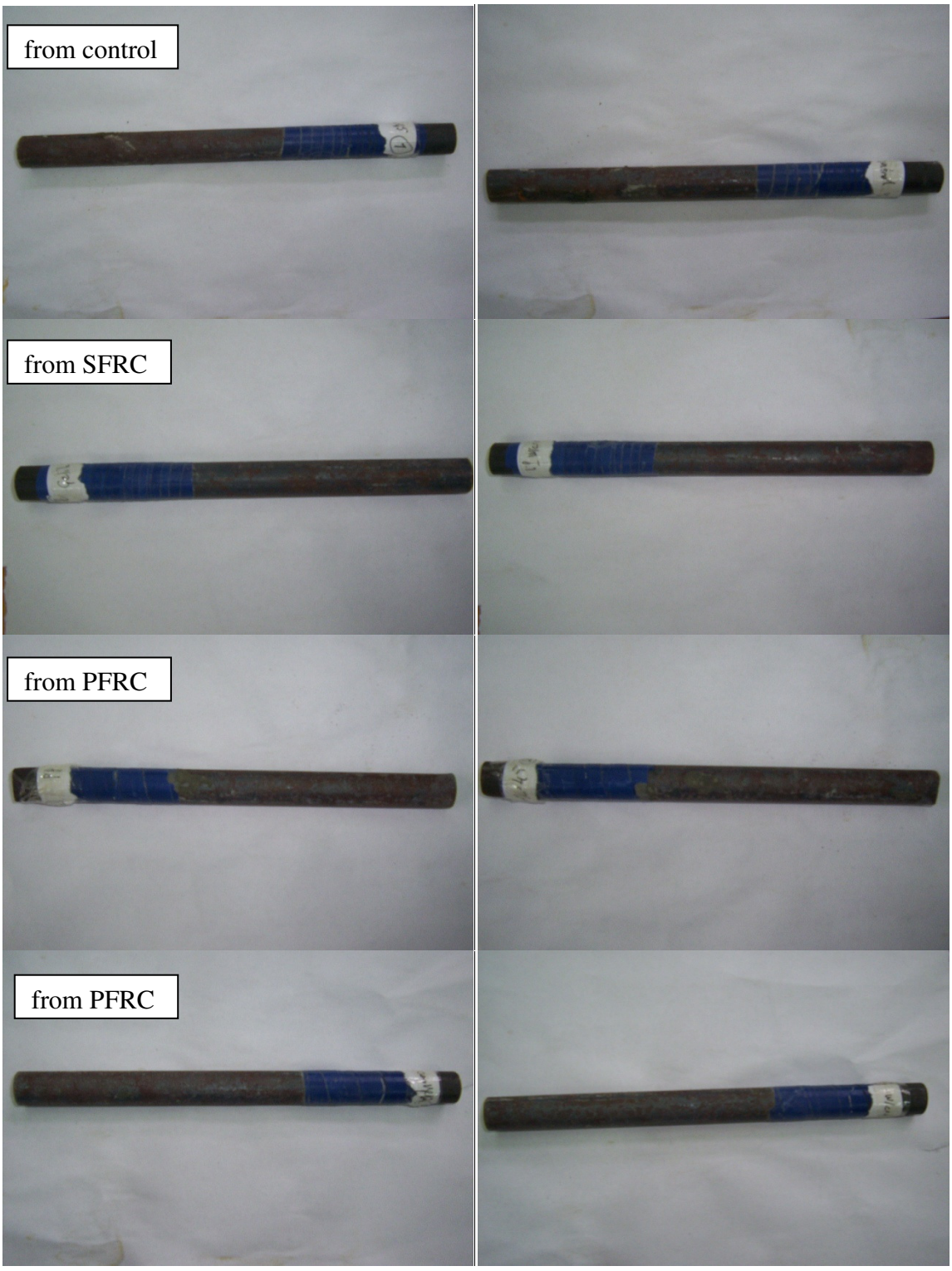

Figure 5.9. Pictures of removed steel bars before cleaning (pictures from opposite sides)

From this section it should be noted that PFRC specimens withstood rebar corrosion product induced internal stresses for longer time duration in comparison to the other tested specimens, despite its relatively lower tensile strength. Also, PFRC rebar mass loss at cracking was found to be the least comparatively. Therefore it is proven that polypropylene fibers delayed the rebar corrosion process and the concrete cover cracking by 82 percent in comparison to the time duration to first crack of control concrete.

5.4.4. Micro-cracking

At the time of first cracking the current may retain a minimum value for some time before significant rise is observed. During this stage the dissolved metal around the rebar has increased the volume around the steel bar, thus applying an internal stress to the concrete cover, at the limit of the concretes energy capacity. The first cracks are locally formed and stress relief can be achieved by their propagation through weak areas of the concrete. The ability of different concretes to delay this stage of cracking is attributed to the ability of retaining micro-cracking. Behavior of FRC during micro-cracking can be studied through the corrosion rate values obtained at cracking, through the time duration that current is kept at a minimum value and through the electrical charge attained during this time duration.

PFRC retains a minimum current at first crack for the longest time compared to the other tested specimens. Observation of the rate of increase of the corrosion going through the specimens, for 20 hours following first crack, it is clear that PFRC it has the smallest rate of increase. The slope obtained during the period of 45 to 65 hours is the smallest in comparison to the corresponding slopes obtained on the other tested specimens. PFRC has a slightly larger slope starting after 100 hours and keeps a steady rate of increase up to the end of the experiment. This observation leads to the conclusion that PFRC has enhanced micro cracking resistance characteristics.

5.4.5. Crack Propagation during accelerated corrosion test

The effect of fibers added to concrete on post cracking, macro-cracking, propagation of the accelerated corrosion induced cracks can be understood by comparison of the total electrical charge passing through the specimens up to completion of the test and by observation of the current-time graph after first crack.

GFRC attained the highest values of charge, over two times higher than control concrete. The charge calculated to have passed through SFRC was 26 percent higher than control concrete. PFRC had the lowest value of total electrical charge during the experiment attaining a 33 percent lower value than control concrete.

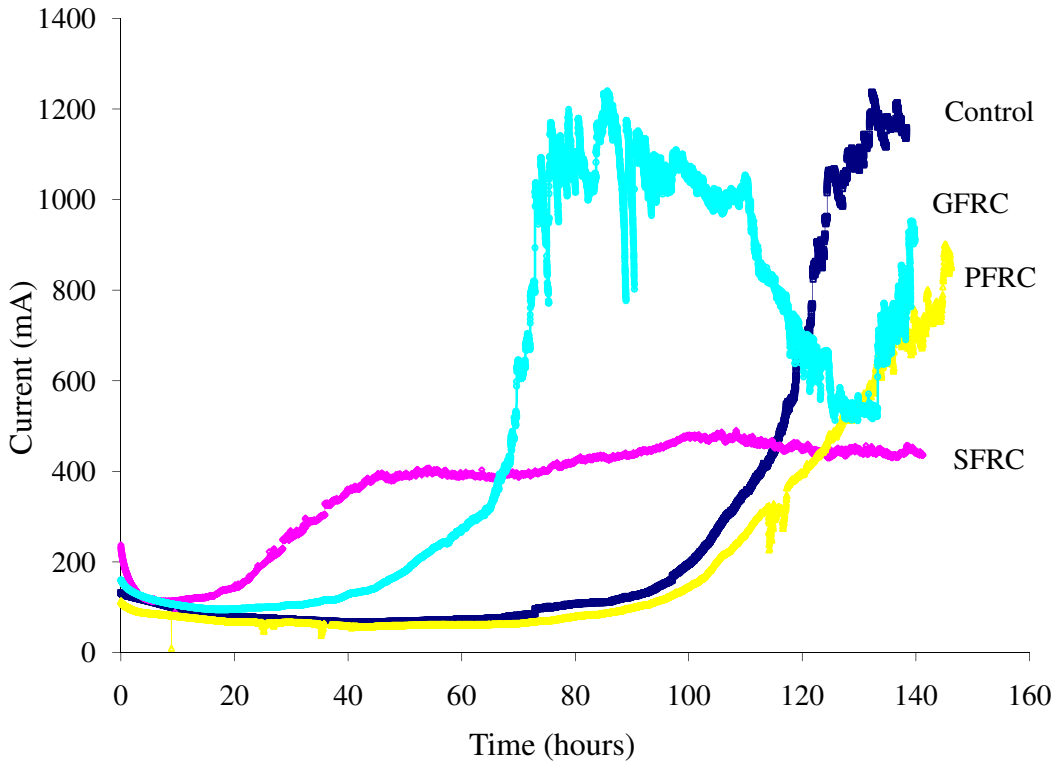

Figure 5.10. Accelerated Corrosion Test Results

The results obtained for accelerated corrosion induced cracking propagation may be correlated to the post peak performance of the FRCs in the flexure test. It was proven that FRC toughness is higher than plain concrete toughness. More specifically, SFRC had reached exceptionally high values of fracture energy, GFRC had a 50 percent higher G_f and PFRC had a 17 percent higher G_f than control concrete. However, the exceptional high fracture energy of SFRC is not correlated with its corresponding electrical charge because of the deviation of the results due to the high steel fiber conductivity. PFRC comparatively lower electrical charge value taking account of its comparatively higher toughness can be said to have good correlation. GFRC accelerated corrosion crack propagation behavior cannot be correlated to the flexure test results.

The slope of the curves after the point of first crack in Figure 5.7 can offer information about the rate of crack propagation. For SFRC, it is observed that the post cracking behavior is the most 'ductile' as, after a steady increase with a smaller slope than the corresponding slope for control concrete, there is maximum corrosion point reached on the curve and retained until the end of the test. Whereas control concrete post cracking behavior is weaker, presenting a steep, steadily increasing slope up to the end of the test. This observation is clearly attributed to the effect of steel fibers, implementing their load resisting capabilities after the cracks initiate. Glass fibers do not appear to have a positive effect on the resistance of propagation of large electrical current induced cracks.

5.4.6. Permeation properties

Impressed potential accelerated corrosion has been reported to provide information on the concrete permeation characteristics. Previous studies [23, 27] reported that improved permeation characteristics of concrete delayed the initial corrosion time and increased the resistance to corrosion cracking, by decreasing the corrosion rate. Apart from accelerated corrosion test the rate of water absorption test conducted in this study also describes the penetrability of FRC.

In this study, the results obtained for initial sorptivity coefficients show a good correlation with the time to first crack, neglecting SFRC due to its unacceptably fast rate of

corrosion. PFRC initial sorptivity coefficient was significantly lower than GFRC and control concrete which behaved similarly. This in conjunction with PFRC delayed time to first crack it could be said that PFRC improved permeation characteristics delay the time of first corrosion induced crack. The alterations caused by glass fibers are insignificant.

6. SUMMARY AND CONCLUSIONS

6.1. Summary

In this study an experimental program was conducted to investigate the effect of fiber addition to concrete mixes on the mechanical properties of concrete, on the rebar corrosion resistance and on the sorptivity of concrete. For this purpose, 0.45 w/c concrete was produced with addition of steel, polypropylene or glass fibers into the casting mix, at fixed volume fractions. Fibers were incorporated into the concrete mix at fixed volume fractions. Steel fibers were 0.5 percent, polypropylene fibers were 0.1 percent and glass fibers were 0.1 percent by volume of concrete. Two different curing regimes were applied to the cast specimens, curing in a water tank or curing in laboratory ambient environmental conditions.

The fiber-reinforced concretes were tested to evaluate and compare their mechanical properties such as compressive strength, splitting tensile strength, rebound number, modulus of elasticity and flexure-toughness. Their performance was further investigated for their durability performance with respect to capaillary surface rate of water absorption and accelerated corrosion testing involving impressed current initiated corrosion of concrete embedded reinforcement. Finally, all test results for FRC were compared with a reference concrete (control specimen) cast without fibers.

6.2. Conclusions

6.2.1 For FRC fresh concrete properties

All concrete mixes were cast with a desired slump of 17 ± 2 cm. This was achieved by using a high range water-reducing admixture. Apart from the fiber addition, all other concrete components are of the same type and the casting and compaction methods were the same for FRC and control concrete. Control concrete has less air content than the FRCs.

6.2.2. For FRC mechanical properties

PFRC and SFRC exhibited a 15 percent higher compressive strength in comparison to control concrete. GFRC compressive strength was negligibly lower than control concrete. The increased air content in GFRC may be the reason for its compressive strength weakness. However, this was not the case for PFRC or SFRC which had higher compressive strength and higher air content than control concrete.

Steel fiber-reinforced concrete produces the highest values of split-tensile strength. In comparison to control concrete SFRC tensile strength was on average increased by 20 percent but there was a case where the increase attained was 58 percent. These results comply with previous research results. GFRC behaved almost the same with SFRC achieving on average high tensile strengths. PFRC on the other side has a lower tensile strength than control concrete. A 15 percent decrease in tensile strength is observed by addition of polypropylene fibers.

In general the SFRC and PFRC modulus of elasticity are not significantly different to plain concrete modulus of elasticity. However, it should be noted that GFRC in this report has a decreased (13 percent lower) modulus of elasticity in comparison to control concrete.

SFRC and GFRC on average withstand a 5 and 7 percent higher maximum load respectively, than control concrete. PFRC, on the other hand, withstands a maximum load which is 5 percent lower than control concrete. The fracture energies (G_f) obtained indicate the higher toughness of FRC in comparison to plain concrete, taking under account the maximum deflection attained and the whole area under the load-deflection curve. SFRC exhibited exceptionally high fracture energy. The G_f of SFRC being 1778.2 kg/sec^2 is over 12 times higher than control concrete. GFRC also produced significantly increased fracture energy, on average 50 percent higher than control concrete. PFRC G_f values are on average 17 percent higher than control concrete.

The flexure-toughness results obtained for the FRC tested in this study generally appear to comply with previous research. SFRC is obviously advantageous in terms of toughness because of its post cracking behavior. The hooked end fibers added to concrete formed mechanical anchors in concrete, bridging the forming cracks which resulted in higher loads retained at larger deflections. It was the only sample that did not break into two separate pieces during the flexural test and the stress was distributed to the broader region.

PFRC has produced a lower flexural stress (5 percent) than control concrete reaching ultimate load at a slightly smaller deflection (3 percent), therefore disagreeing with the improved flexural characteristics reported in [9]. However, PFRC produced improved toughness characteristics withstanding a 43 percent higher maximum deflection than control concrete; results complying with those in [58].

6.2.3. For FRC permeation characteristics

It is clearly observed that fiber addition appears to reduce the rate of water absorption of concrete. The control specimens produce the highest sorptivity coefficient values. Steel fibers have reduced the sorptivity the most, and then polypropylene fibers and finally glass fibers, which also reduced the rate of water absorption but, comparatively, the least. The same result is reached for both water cured and non cured FRC specimens.

Further, the water cured FRC have a significantly lower water absorption rate than non cured FRC.

Cured SFRC initial absorption rates were 12 percent lower than control concrete. Non cured SFRC produce an initial absorption rate on average 26 percent lower than control concrete.

Polypropylene fibers also reduced the rate of water absorption of concrete. Cured PFRC initial absorption rates were up to 10 percent lower than cured control concrete. Non cured PFRC initial sorptivity coefficients were 15 percent lower than control non cured concrete.

Glass fibers produced the least reduction of initial sorptivity coefficients in comparison to the other fibers used. Cured GFRC produces a negligible average of 0.3 percent lower initial water absorption rate than control concrete. However the few specimens tested and the variation of the results do not allow for a clear understanding of the cured GFRC initial water absorption behavior. The non cured GFRC have an initial sorptivity coefficient up to 14 percent lower than control concrete.

SFRC exhibited the less water absorptive behavior at advanced levels of elapsed time in comparison to PFRC and GFRC, whose behaviors were similar, for both curing conditions. As in the initial phase SFRC continued to absorb less water than PFRC and GFRC. It is obtained that during the secondary phase FRC absorbs less water than plain concrete. Comparing to plain concrete results obtained for cured SFRC, GFRC and PFRC were 32, 29 and 31 percent, respectively, lower than cured plain concrete. For non-cured SFRC, GFRC and PFRC results were 21, 12 and 12 percent, respectively, lower than non-cured plain concrete.

Results obtained show that despite the increase in the concrete air content by addition of fibers the rate of water absorption decreases. Also, between different FRC specimens, specimens with higher air content exhibit higher sorptivity coefficients. Further, by comparing the different sorptivity coefficients derived for the different FRCs and their air content percentage, it is understood that a relationship between FRCs air

content and water absorption exists. SFRC has the least air content compared to the other FRC and exhibits the least water absorption. GFRC on the other hand has the highest air content and the highest rate of water absorption in comparison to SFRC and PFRC.

6.2.4. From accelerated corrosion test

The first current passing through SFRC was clearly higher than the other tested specimens. There is reason to believe that the steel fiber electrical resistivity allows higher current to pass through the SFRC cover. Therefore the results obtained for SFRC from the impressed voltage accelerated corrosion test are affected by a parameter which further accelerates the test. This characteristic of SFRC opposes its use in structures where stray currents may be picked up, i.e. railway bridges or tunnels.

Values of first current going through each specimen are decisive for the time needed for the cover crack initiation. In comparison of the elapsed time up to the first crack and the first current read for each specimen it is observed that they are inversely proportional. SFRC with the highest first current reading and therefore the least cover concrete resistance withstands first crack for a shorter time than the other specimens that crack one at a time in an ascending order according to their initially obtained cover resistances.

It is proved that polypropylene fibers delayed the rebar corrosion process and the concrete cover cracking by 82 percent in comparison to the time duration to first crack of control concrete. PFRC specimens withstood rebar corrosion product induced internal stresses for longer time duration in comparison to the other tested specimens, despite its relatively lower tensile strength. Also, PFRC rebar mass loss at cracking was found to be the least comparatively.

GFRC and PFRC appear to resist the micro-cracking of the concrete cover at immediate stages after first crack appearance more than control concrete and SFRC. For duration of 20 hours after the first sign of a significant increase of the rate of corrosion PFRC had the smallest rate of increase of current going through it.

Steel fiber addition to concrete exhibits an advantageous behavior towards the deterioration caused to concrete due to corrosion of the embedded reinforcement. For SFRC, it is observed that the post cracking behavior is the most ‘ductile’ as, after a steady increase with a smaller slope than control concrete, there is a maximum current point reached on the curve and that value is retained up to the end of the test. Whereas control concrete post cracking behavior is weak, presenting a steep, steadily increasing slope up to the end of the test and therefore a faster rate of crack propagation. This SFRC behavior during crack propagation of the accelerated corrosion test is clearly attributed to the effect of steel fibers, implementing their crack arresting capabilities after the cracks initiate.

PFRC initial sorptivity coefficient was significantly lower than GFRC and control concrete which behaved similarly. Also, PFRC delayed time to first crack in the accelerated corrosion test. So it is proved that PFRC improved permeation characteristics delay the time of first corrosion induced crack. The alterations caused by glass fibers are insignificant.

7. FUTURE RESEARCH RECOMMENDATIONS

Impressed current accelerated corrosion testing may be the most accelerated corrosion test enabling laboratory investigations of the corrosion process in new concepts in the concrete industry like FRC, but its capability of reflecting the actual corrosion process most usually initiated by the ingress of aggressive agents like chloride, may depend on the material properties of the concrete mix constituents, together with the fiber material properties, rather than on the permeation properties of the FRC. Therefore further experimentation on FRC is recommended with chloride initiating corrosion methods together with further investigations of their permeation properties at deeper parts within the cover. Microscope inspection of pores or other methods of understanding the pore blocking capabilities of fibers are recommended.

Also, an investigation of the fiber-concrete bond properties would add useful information to the current research. Fiber pullout tests may be performed in order to achieve this and it is recommended to use various fiber aspect ratios.

Further, FRC may be cracked and then corrosion tests may be performed on specimens cored from the cracked FRC. As the major effect of fiber addition to concrete is the crack arresting capability and the corrosion process is aided by the formation and propagation of cracks, it would be interesting to obtain durability characteristics of FRC at different stages of cracking.

APPENDIX A: PHOTOS OF TEST SETUP

Figures A.1, A.2. Actual Setup of Accelerated Corrosion Test

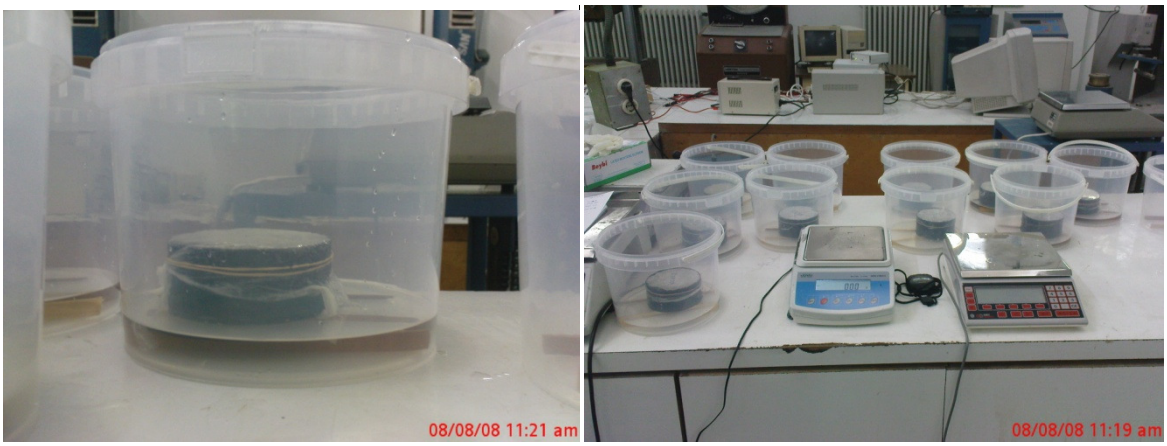

Figure A.3. Sorptivity Test Setup. Left: Specimen exposed to water; right: Working area and equipment used

Figure A.4. Sorptivity Test Procedure. Removal of excess water; Weighing of specimen at specific time intervals

APPENDIX B: SORPTIVITY RESULTS

Table B.1. Absorption I (mm) for Control Concrete and SFRC

Hours	K45C1	K45C2	K45N1	K45N2	S45C1	S45N1	S45C2	S45N2
0	0	0	0	0	0	0	0	0
8	0.28252	0.14949	0.26286	0.24717	0.09172	0.10937	0.10446	0.10847
17	0.33171	0.21466	0.35638	0.38026	0.14395	0.17499	0.14522	0.16901
24	0.36450	0.25682	0.51056	0.41322	0.18217	0.21617	0.14522	0.19423
35	0.40486	0.30793	0.57627	0.43096	0.21401	0.25992	0.17325	0.24342
42	0.44522	0.34498	0.61924	0.53870	0.24459	0.29595	0.21019	0.28378
60	0.51711	0.42676	0.71276	0.63123	0.30701	0.37958	0.23312	0.36702
85	0.59152	0.50086	0.80122	0.76306	0.37962	0.47995	0.30064	0.45279
104	0.64449	0.55197	0.88336	0.85939	0.43567	0.56101	0.37070	0.52846
120	0.69368	0.60564	0.92760	0.93164	0.47516	0.61505	0.47389	0.58017
134	0.74035	0.63886	1.00595	1.00262	0.50955	0.67424	0.51210	0.63062
147	0.90557	0.68486	1.02364	1.05079	0.54777	0.70255	0.53248	0.66215
304	1.14647	1.02601	1.42425	1.59837	0.79745	1.07956	0.80892	1.03296
440	1.38989	1.23555	1.65931	1.91272	0.94650	1.31631	0.97707	1.25494
518	1.53871	1.36588	1.80211	2.16242	1.02803	1.46815	1.06115	1.37728
657	1.74304	1.53326	1.99294	2.37030	1.12484	1.63027	1.14904	1.50718
726	1.80610	1.58437	2.05866	2.42227	1.15541	1.67917	1.17834	1.55007
789	1.84520	1.62909	2.09404	2.45269	1.17197	1.69847	1.18981	1.57277
831	1.86664	1.64825	2.12437	2.47043	1.18726	1.71262	1.20000	1.59169

Table B.2. Absorption I (mm) for GFRC and PFRC

Hours	G45C1	G45N1	G45N2	G45C2	P45N1	P45C1	P45C2	P45N2
0	0	0	0	0	0	0	0	0
8	0.09488	0.11465	0.11083	0.10918	0.13257	0.11099	0.13121	0.15207
17	0.14687	0.19490	0.18217	0.18197	0.19236	0.15639	0.18471	0.21706
24	0.18456	0.24713	0.23312	0.21966	0.23006	0.18414	0.21401	0.25215
35	0.22616	0.29809	0.28662	0.23915	0.27945	0.22198	0.25605	0.30804
42	0.25605	0.34268	0.33376	0.31064	0.31974	0.24720	0.28153	0.34573
60	0.32494	0.44459	0.43694	0.38473	0.41462	0.31279	0.35032	0.43802
85	0.39902	0.55159	0.55287	0.47441	0.52900	0.40360	0.42930	0.55239
104	0.46011	0.64204	0.64841	0.54330	0.61868	0.45783	0.49172	0.64338
120	0.49261	0.69809	0.70701	0.58749	0.68497	0.49819	0.53758	0.70836
134	0.53810	0.75924	0.78217	0.63298	0.74476	0.53477	0.57707	0.76425
147	0.55759	0.79618	0.82293	0.65507	0.78375	0.55621	0.59490	0.80844
304	0.83444	1.22803	1.25860	0.99041	1.23216	0.82611	0.87771	1.26076
440	0.98911	1.48408	1.52357	1.15028	1.51811	0.98755	1.02675	1.53371
518	1.06710	1.63057	1.68917	1.24126	1.66498	1.06575	1.10446	1.68838
657	1.16068	1.79236	1.89045	1.34654	1.84695	1.16917	1.20000	1.88464
726	1.18017	1.95669	1.93631	1.37644	1.88854	1.18935	1.22038	1.92103
789	1.19577	1.85350	1.95796	1.39333	1.91063	1.21205	1.23694	1.92753
831	1.20877	1.86624	1.97452	1.40633	1.91973	1.22214	1.24713	1.94053

Note: Rate of Absorption with R^2<0.98 does not allow for a sorptivity coefficient to be obtained. Initial and secondary sorptivity coefficients are derived from the first and second curve respectively.

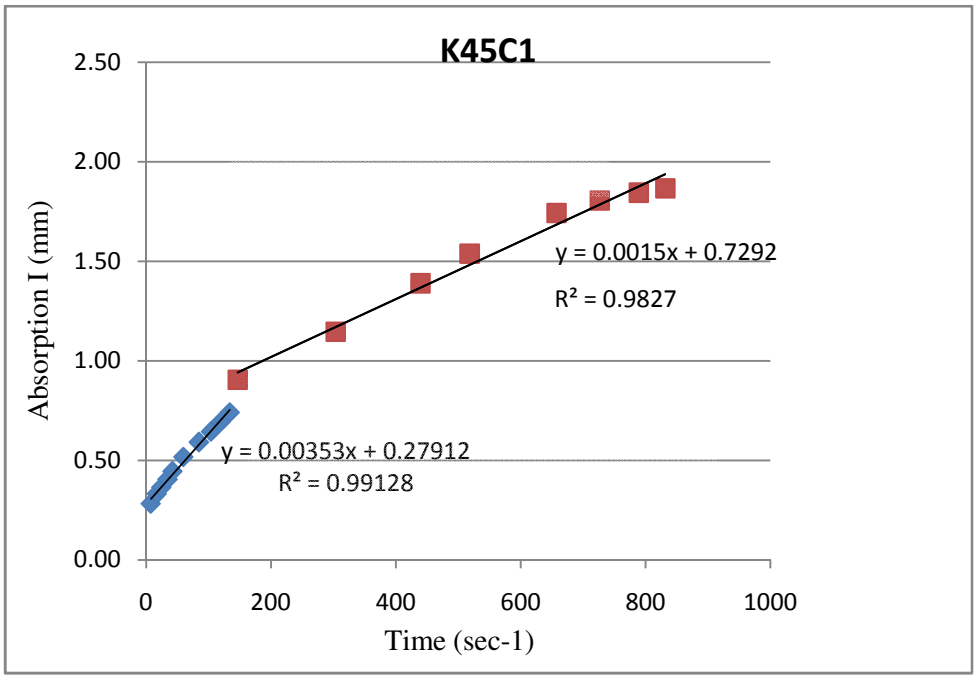

Figure B.1. Rate of Water Absorption of K45C1

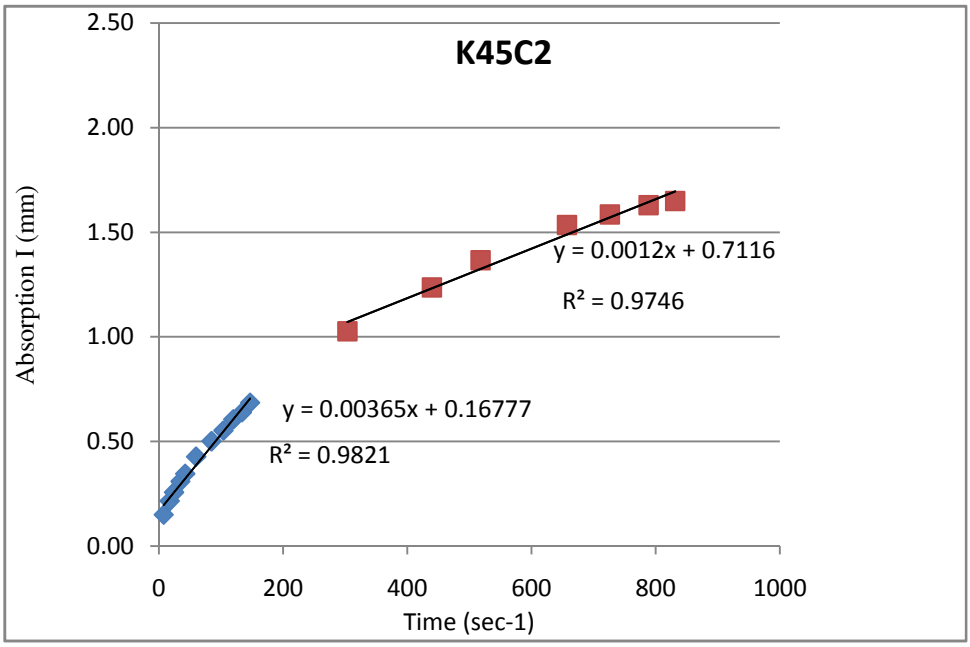

Figure B.2. Rate of Water Absorption of K45C2

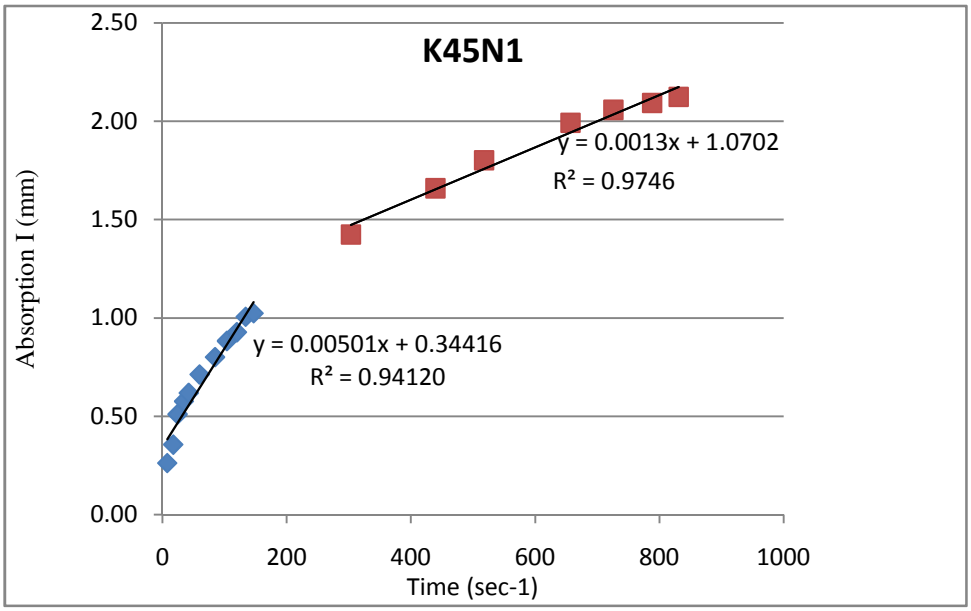

Figure B.3. Rate of Water Absorption of K45N1

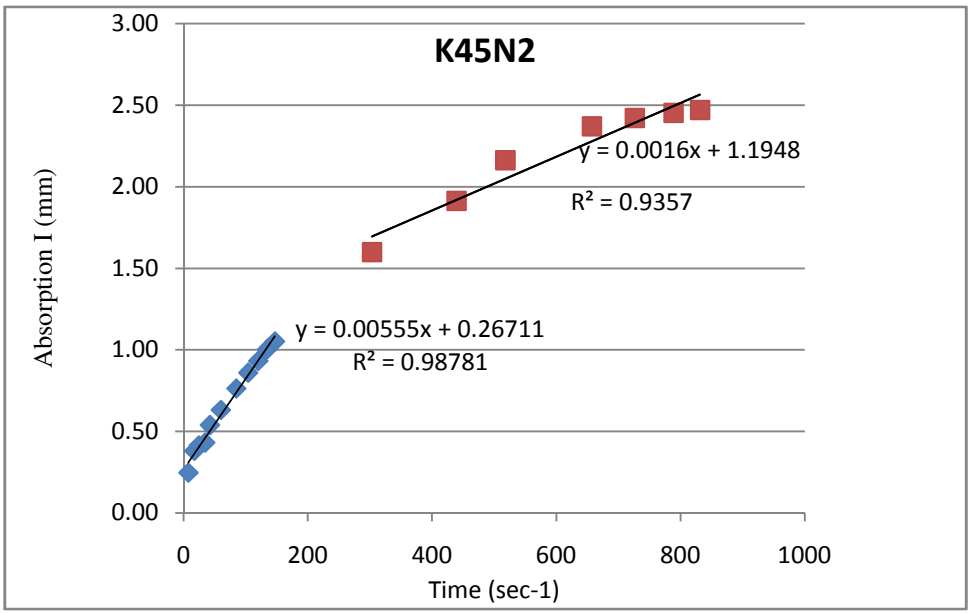

Figure B.4. Rate of Water Absorption of K45N2

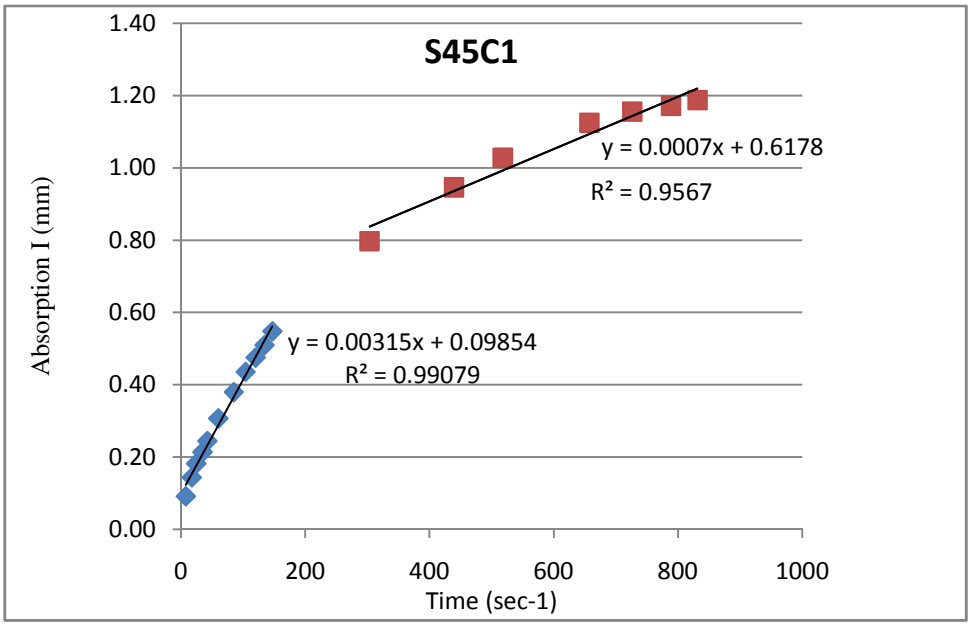

Figure B.5. Rate of Water Absorption of S45C1

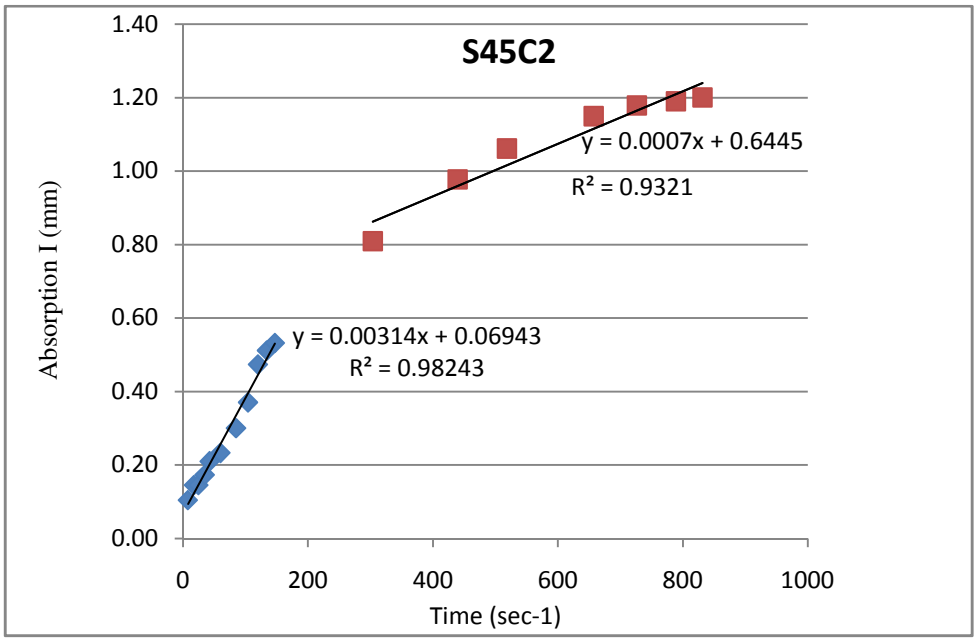

Figure B.6. Rate of Water Absorption of S45C2

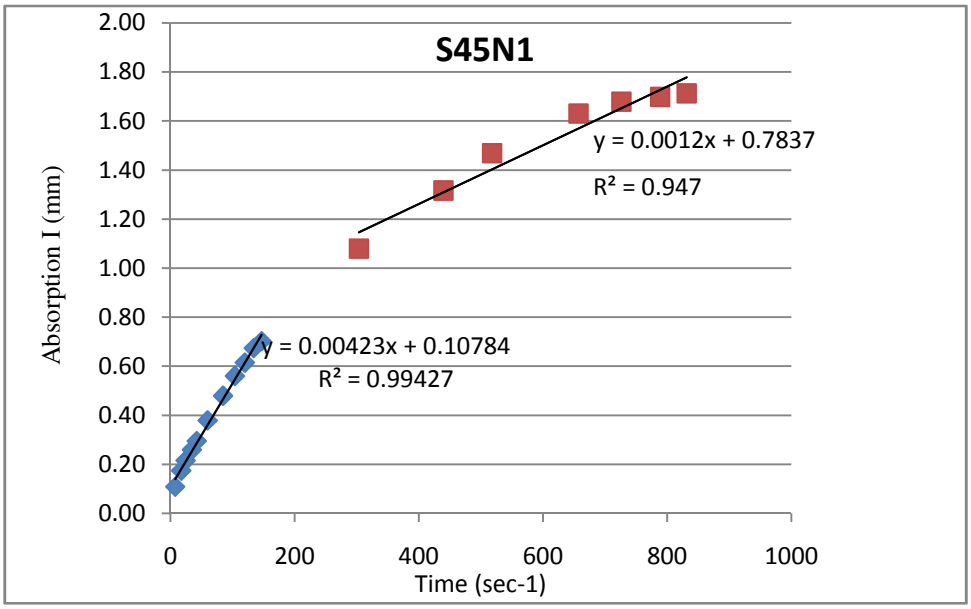

Figure B.7. Rate of Water Absorption of S45N1

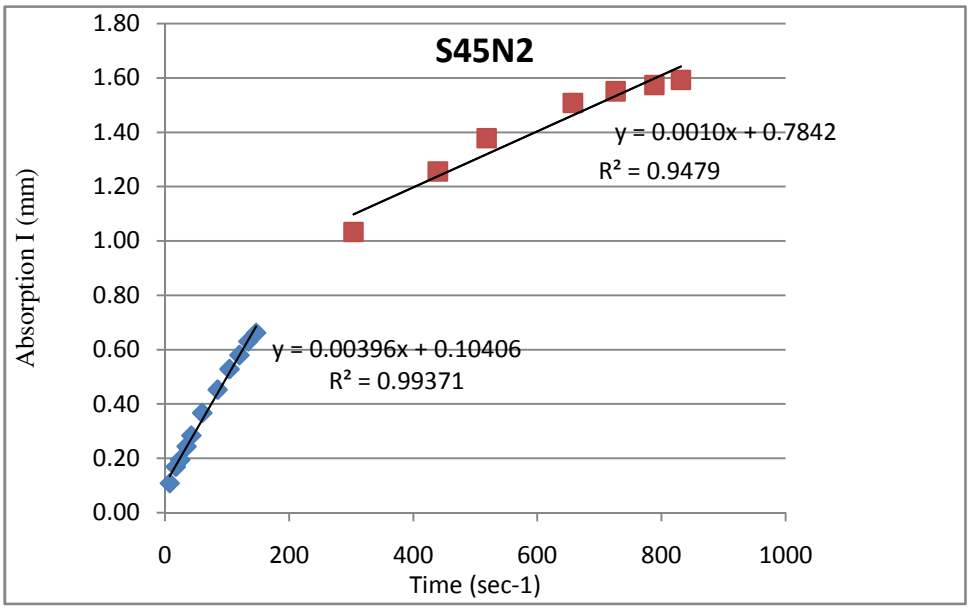

Figure B.8. Rate of Water Absorption of S45N2

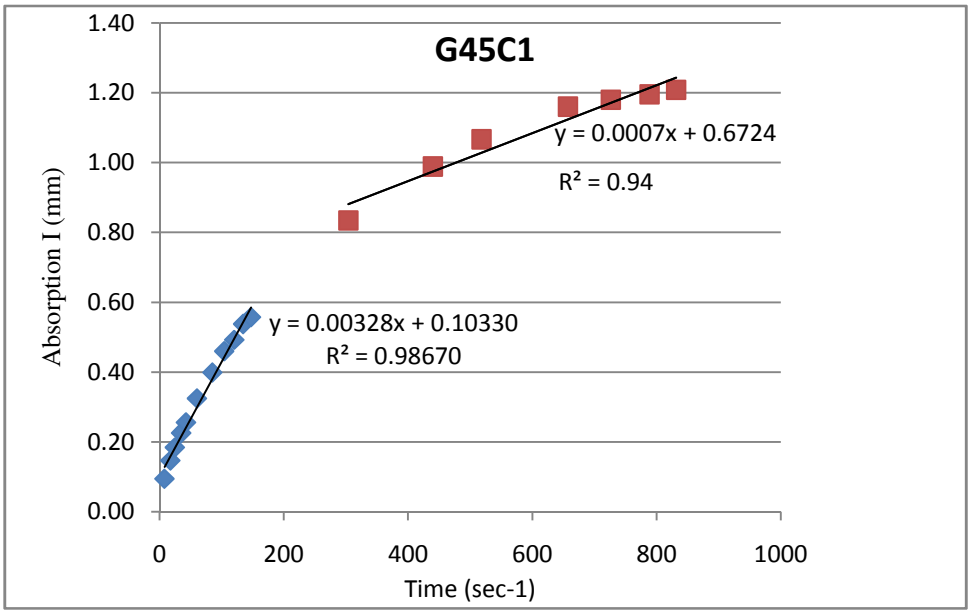

Figure B.9. Rate of Water Absorption of G45C1

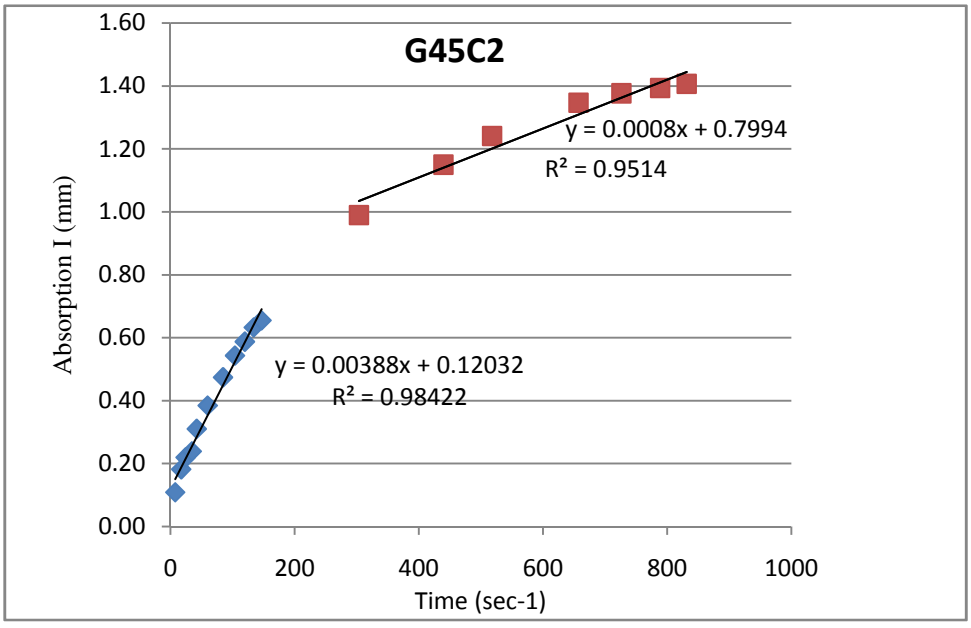

Figure B.10. Rate of Water Absorption of G45C2

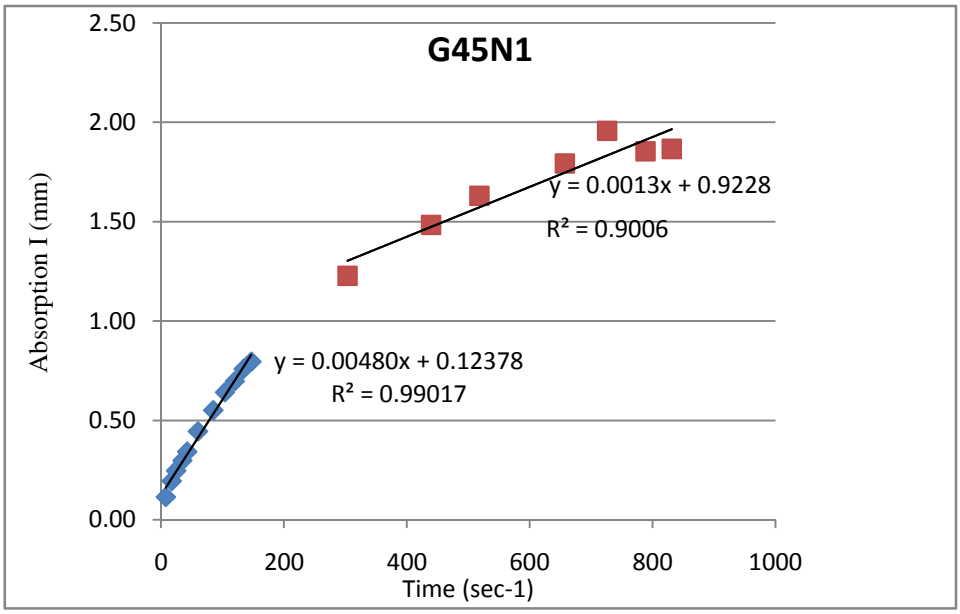

Figure B.11. Rate of Water Absorption of G45N1

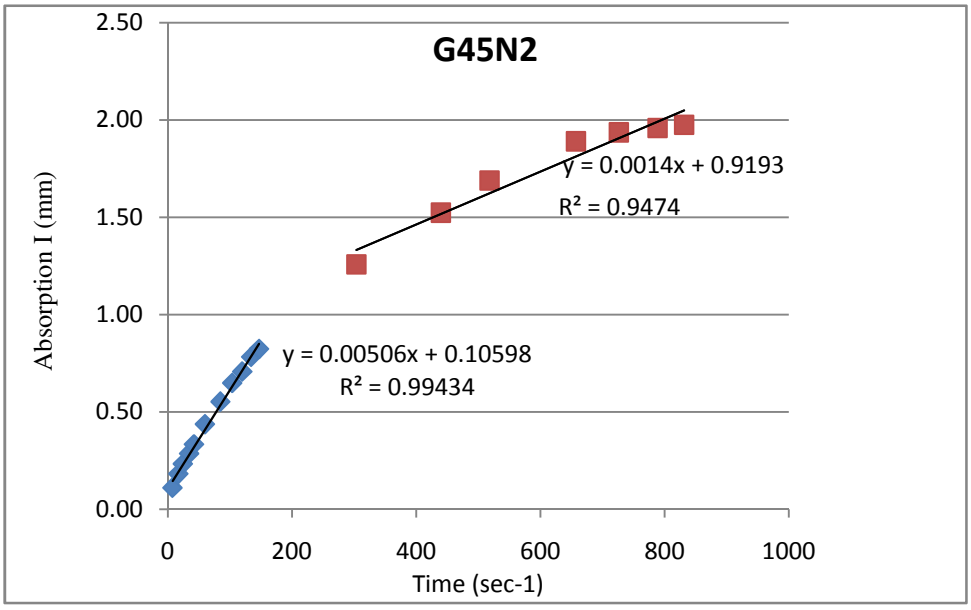

Figure B.12. Rate of Water Absorption of G45N2

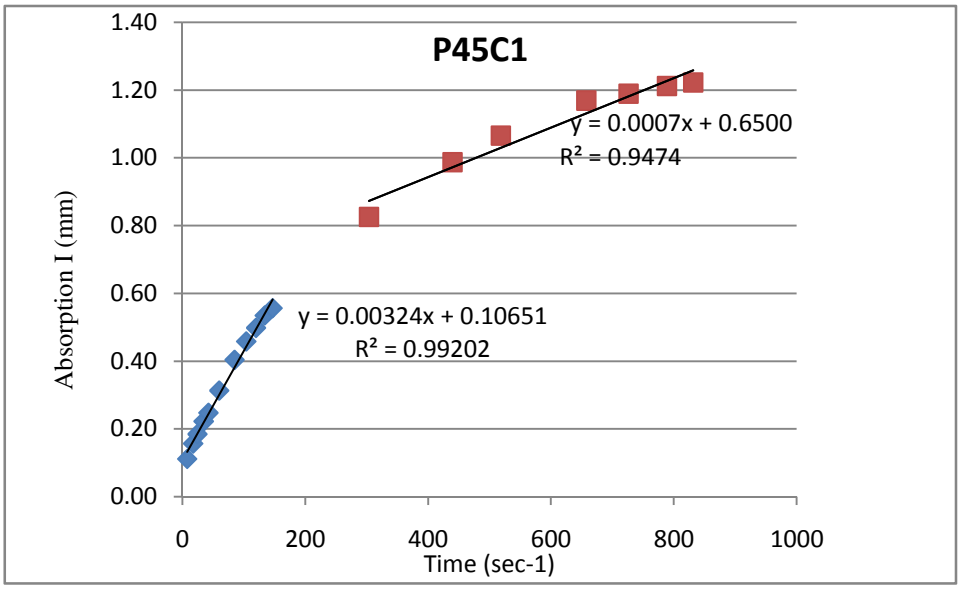

Figure B.13. Rate of Water Absorption of P45C1

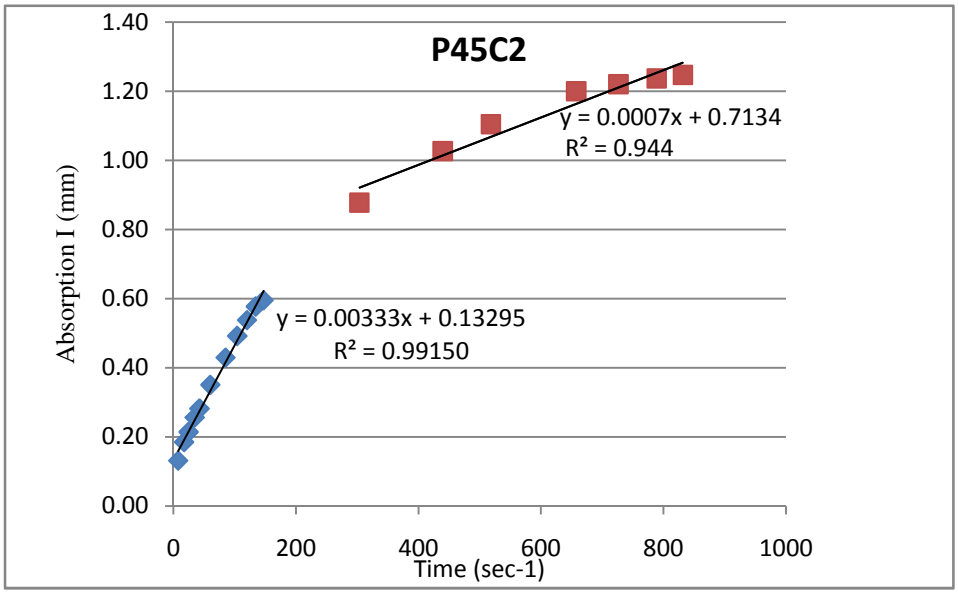

Figure B.14. Rate of Water Absorption of P45C2

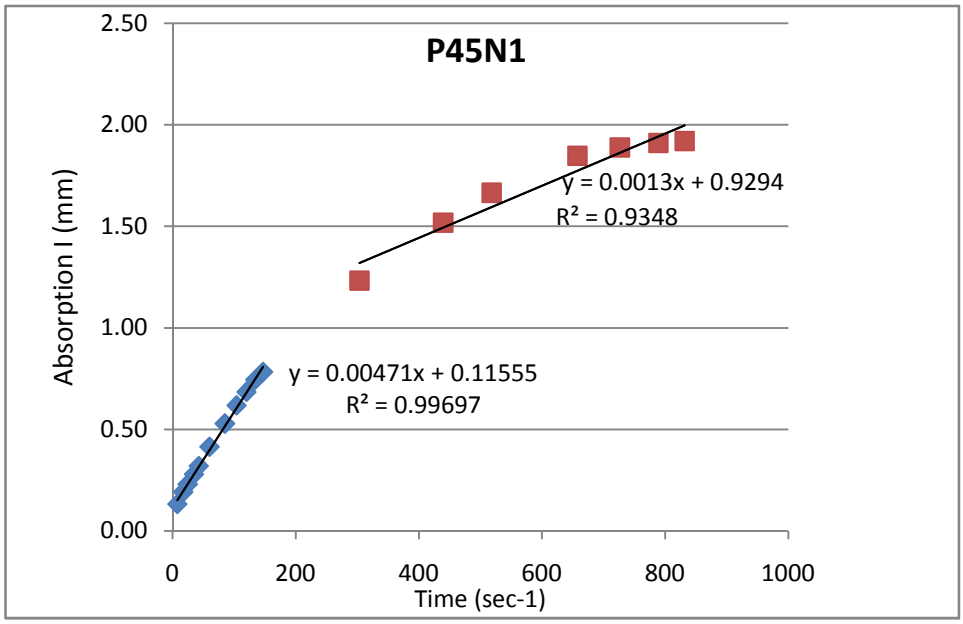

Figure B.15. Rate of Water Absorption of P45N1

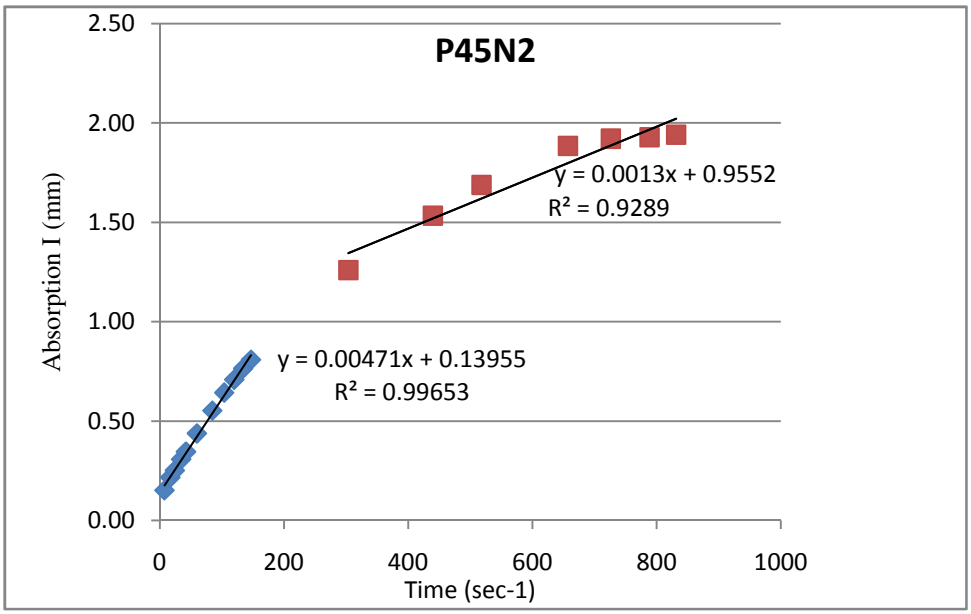

Figure B.16. Rate of Water Absorption of P45N2

Table B.3. Initial Sorptivity Coefficients

	Initial Sorptivity Coefficients ($cm/s^{1/2}$)
K45C1	0.00353
K45C2	0.00365
Average	0.00359
K45N1	0.00501
K45N2	0.00555
Average	0.00528
S45C1	0.00315
S45C2	0.00314
Average	0.00315
S45N1	0.00423
S45N2	0.00396
Average	0.00410
G45C1	0.00328
G45C2	0.00388
Average	0.00358
G45N1	0.00480
G45N2	0.00506
Average	0.00493
P45C1	0.00324
P45C2	0.00333
Average	0.00329
P45N1	0.00471
P45N2	0.00471
Average	0.00471

Table B.4. R-squared of Initial Sorptivity trend line

	C1	C2	N1	N2
SFRC	0.9908	0.9824	0.9943	0.9937
GFRC	0.9867	0.9842	0.9902	0.9943
PFRC	0.9920	0.9915	0.9970	0.9965
Control	0.9913	0.9820	**0.9412**	0.9878

Table B.5. R-squared of Secondary Sorptivity trend line

	C1	C2	N1	N2
SFRC	**0.9560**	**0.9320**	**0.9470**	**0.9470**
GFRC	**0.9400**	**0.9510**	**0.9000**	**0.9470**
PFRC	**0.9470**	**0.9440**	**0.9340**	**0.9280**
Control	0.9820	**0.9740**	**0.9740**	**0.9350**

APPENDIX C: MASS LOSS AND CORROSION DAMAGE ASSESMENT

Table C.1. Mass Loss (grams)

	Before	After Treatment (acid)		
	(grams)		Loss (grams)	time (hour)
Control	341.79	340.20	1.59	45.5
	329.55	292.52	37.03	146.5
SFRC	323.19	321.73	1.46	24.0
	321.75	287.74	34.01	146.5
PFRC	323.71	322.51	1.20	45.5
	316.02	297.02	19.00	146.5
GFRC	326.65	325.3	1.35	26.5
	325.57	239.99	85.58	146.5

Figure C.1. Specimens at first crack (left); at the end of experiment (right)

Figure C.2. Corrosion Damage. Steel bars after cleaning. Obtained from control concrete, SFRC, PFRC and GFRC from left to right (a) at first crack and (b) at the end of accelerated corrosion test

APPENDIX D: FLEXURE TEST RESULTS

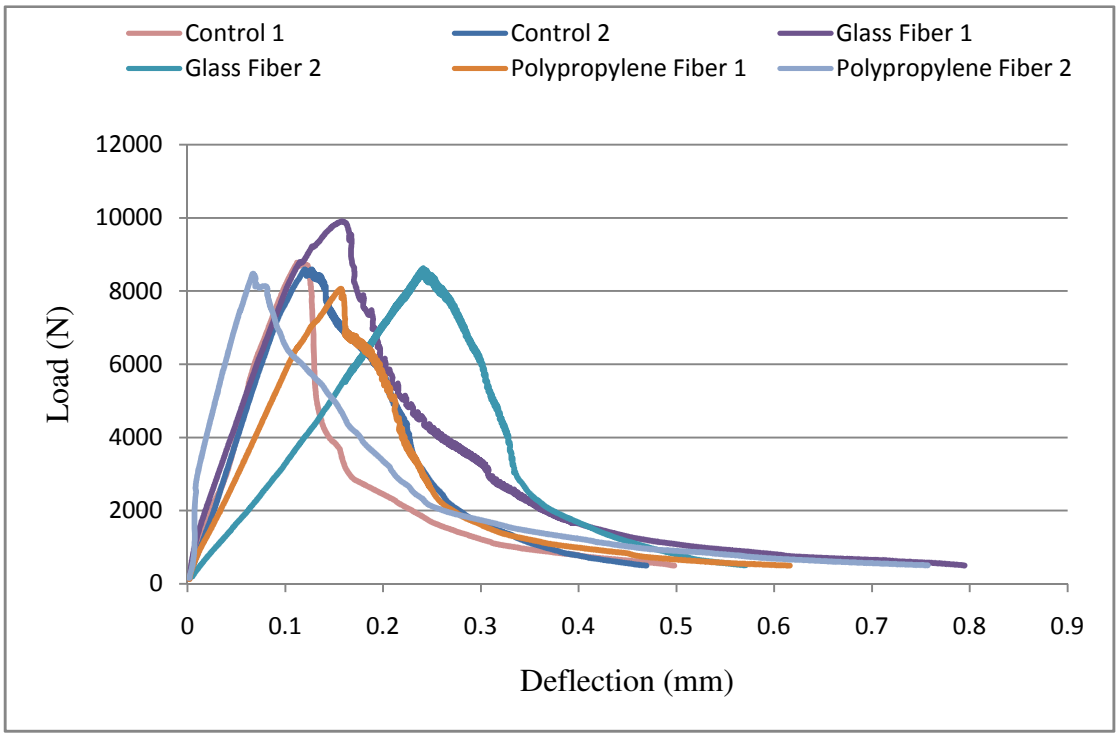

Figure D.1. Flexural Load-Deflection graph for GFRC, PFRC and control concrete

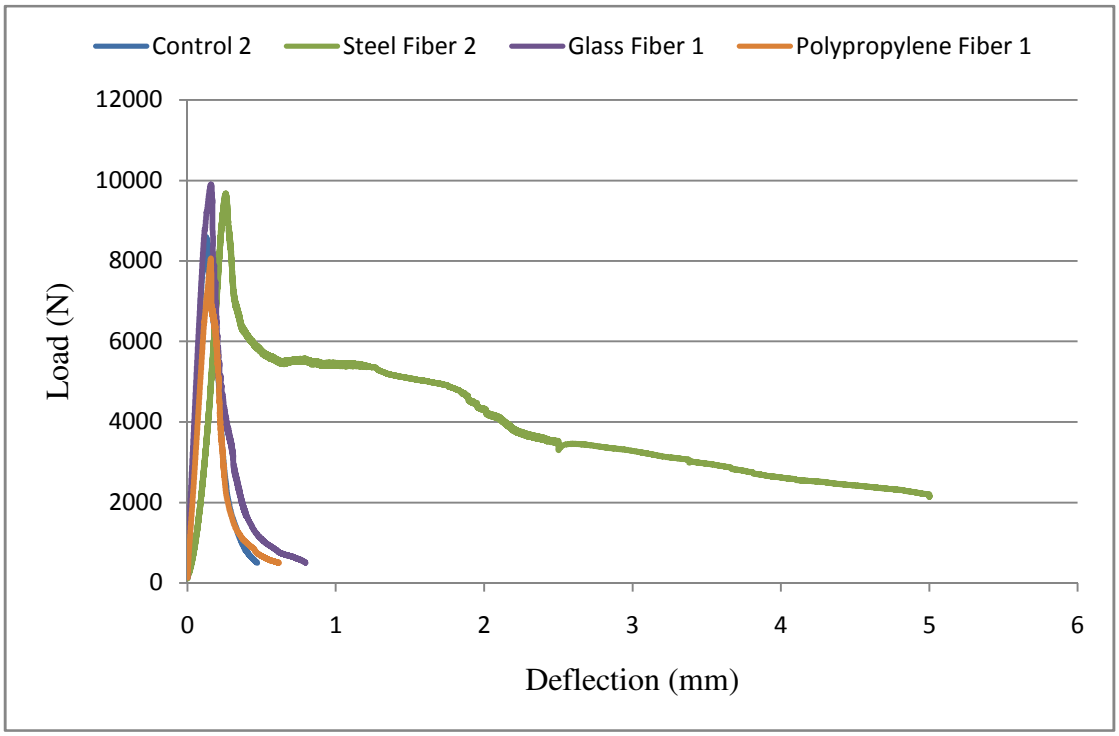

Figure D.2. Flexural Load-Deflection graph for SFRC, GFRC, PFRC and control concrete

REFERENCES

1. ACI Committee 544, "State-of-the-Art Report on Fiber Reinforced Concrete", *American Concrete Institute*, ACI 544.1R-96, Detroit, Michigan, 1996.

2. ACI Committee 544, "Measurement of Properties of Fiber Reinforced Concrete", *ACI Materials Journal*, ACI 544.2R-89, Title no.85-M58, 1998.

3. Balaguru, P. N. and S. P. Shah, *Fiber-Reinforced Cement Composites*, McGraw-Hill Inc., 1992.

4. Swamy, R. N., P. S. Mangat, and C. V. S. K. Rao, "The Mechanics of Fiber Reinforcement of Cement Matrices", *An Int. Symposium: Fiber Reinforced Concrete*, ACI Publication SP-44, Detroit, pp.1-28, 1973.

5. Karbhari, V. M., J. W. Chin, D. Hunston, B. Benmokrane, T. Juska, R. Morgan, J. J. Lesko, U. Sorathia and D. Reynaud, "Durability Gap Analysis for Fiber-Reinforced Polymer Composites in Civil Infrastructure", *Journal of Composites for Construction*, DOI: 10.1061/(ASCE)1090-0268(2003)7:3(238), 2003.

6. Broomfield, J. P. *Corrosion of Steel in Concrete*, E & F Spon, Chapman and Hall, London, 1997.

7. Aldred, J. M., "Hydrophobic pore blocking ingredient improves concrete durability", *Concrete International*, November, 1988.

8. McCarter W.J., "Influence of Surface Finish on Sorptivity of Concrete", *Journal of Materials in Civil Engineering*, Vol. 5, No. 1, February, 1993.

9. Altun F., T. Haktanir and K. Ari, "Effects of steel fiber addition on mechanical properties of concrete and RC beams", *Construction and Building Materials*, Vol. 21, pp. 654–661, 2007.

10. Mohammadi, Y., P. S. Singh and S. K. Kaushik, "Properties of steel fibrous concrete containing mixed fibres in fresh and hardened state", *Construction and Building Materials*, Vol. 22, pp. 956–965, Elsevier, 2008.

11. Sivakumar, A. and M. Santhanam, "Mechanical properties of high strength concrete reinforced with metallic and non-metallic fibers", *Cement & Concrete Composites*, Vol. 29, pp. 603-608, 2007.

12. Köksal, F., A. İlki, F. Bayramov and M.A. Taşdemir, "Deformation and Fracture of Steel Fiber Reinforced Concretes", *Sixth International Congress on Advances in Civil Engineering*, Bogazici University, Istanbul, Turkey, 6-8 October, 2004.

13. Toutanji, H., S. McNeil and Z. Bayasi, "Chloride permeability and impact resistance of polypropylene-fiber-reinforced silica fume concrete", *Cement and Concrete Research*, Vol. 28, pp. 961-968, 1998.

14. Hsie, M., C. Tu and P.S. Song, "Mechanical properties of polypropylene hybrid fiber-reinforced concrete", *Materials Science and Engineering*, A 494, pp. 153–157, 2008.

15. Toutanji, H., "Properties of polypropylene fiber reinforced silica fume expansive-cement concrete", *Construction and Building Materials*, 13(1999):171-177, Elsevier, 1999.

16. Swamy, R. N. and H. Stavrides, "Influence of Fiber Reinforcement on Restrained Shrinkage and Cracking", *ACI Journal*, Title No. 76-21, March, 1979.

17. Bayasi, Z. and J. Zeng, "Properties of Polypropylene Fiber Reinforced Concrete", *ACI Materials Journal*, Vol. 90, No. 6, pp. 605-610, November-December, 1993.

18. Myers, D., T. H. K. Kang and C. Ramseyer, "Early-Age Properties of Polymer Fiber-Reinforced Concrete", *International Journal of Concrete Structures and Materials*, Vol. 2, No. 1, pp. 9-14, June, 2008.

19. Al-Tayyib, A. H. and M. M. Al-Zahrani, "Corrosion of steel Reinforcement in Polypropylene Fiber Reinforced Concrete Structures", *ACI Materials Journal*, Title no. 87-M12, March-April, 1990.

20. Takagi J., "Some Properties of Fiber Reinforced Concrete", *An Int. Symposium: Fiber Reinforced Concrete*, ACI Publication SP-44, Detroit, pp.93-111, 1974.

21. Marsh H. N. and L. L. Jr. Clarke, "Glass Fiber Reinforced Cement Base Materials", *An Int. Symposium: Fiber Reinforced Concrete*, ACI Publication SP-44, Detroit, pp.247-264, 1974.

22. Proctor, B. A. and B. Yale, "Glass Fibres for Cement reinforcement". *Philosophical Transactions of the Royal Society of London*, Series A, Mathematical and Physical Sciences, A294, pp.427-436, Great Britain, 1980.

23. Shah, S.P., D. Ludirdja, J. I. Daniel and B. Mobasher, "Toughness-Durability of Glass Fiber Reinforced Concrete Systems", *ACI Materials Journal*, Title no. 85-M39, September-October, 1988.

24. Topçu, İ. E. and M. Canbaz, "Effect of different fibers on the mechanical properties of concrete containing fly ash", *Construction and Building Materials*, Vol. 21, pp. 1486-1491, 2007.

25. Puertas, F., T. Amat, A. Fernandez-Jimenez and T. Vazquez, "Mechanical and durable behavior of alkaline cement mortars reinforced with polypropylene fibers", *Cement and Concrete Research*, Vol. 33, pp. 2031–2036, Elsevier Ltd, 2003.

26. Gopalaratnam, V.S., P. S. Shah, G. B. Ramakrishnan and M. Wecharatana, "Fracture toughness of fiber reinforced concrete", *AC1 Materials Journal*, Vol. 88 (4), pp. 339-353, July-August, 1991.

27. Banthia, N. and J-F. Trottier, "Test Methods for Flexural Toughness Characterization of Fiber Reinforced Concrete: Some Concerns and a Proposition", *ACI Materials Journal*, Vol. 92 (1), January-February, 1995.

28. Barros, J.A.O. and J.A. Figuerios, "Flexural Behaviour of SFRC: Testing and Modelling", *Journal of Material in Civil Engineering*, Vol. 11, No.4, pp. 331-339, 1999.

29. Ezeldin, A. S. and P. N. Balaguru, "Normal and High Strength Fiber Reinforced Concrete under Compression", *Journal of Materials in Civil Engineering*, Vol. 4, No. 4, November, 1992.

30. Balaguru, P. N., R. Narahari and M. Patel, "Flexural Toughness of Steel Fiber Reinforced Concrete", *ACI Materials Journal*, Vol. 89, No.6, pp. 541-545, November-December, 1992.

31. Marikunte, S., C. Aldea and S. P. Shah, "Durability of Glass Fiber Reinforced Cement Composites: Effect of Silica Fume and Metakaolin", *Advanced Cement Based Materials*, 1997; 5, pp.100-108, Elsevier Science, 1997.

32. Wheat, H. G., "Using polymers to minimize corrosion of steel in concrete", *Cement & Concrete Composites*, Vol. 24, pp. 119-126, 2002.

33. Basheer, L., J. Kropp and D. J. Cleland, "Assessment of the durability of concrete from its permeation properties: a review", *Construction and Building Materials*, Vol. 15, pp. 93-103, Elsevier Science Ltd, 2001.

34. Williamson G. S., R. E. Weyers, M. C. Brown, A. Ramniceanu and M. M. Sprinkel, "Validation of Probability-Based Chloride-Induced Corrosion Service-Life Model", *ACI Materials Journal*, Vol. 105, No. 4, July-August, 2008.

35. Claisse, P. A., H. I. Elsayad and G. Shaaban, "Absorption and Sorptivity of Cover Concrete", *Journal of Materials in Civil Engineering*, pp.105-110, August, 1997.

36. McCarter W.J. “Influence of Surface Finish on Sorptivity of Concrete”, *Journal of Materials in Civil Engineering*, Vol. 5, No. 1, February, 1993.

37. Wang, K., C. Jansen, and P. S. Shah., “Permeability Study of Cracked Concrete”, *Cement and Concrete Research*, Vol. 27, No. 3, pp. 381-393, Elsevier Science Ltd, 1997.

38. Hall, C., “Water Sorptivity of Mortars and Concretes: A Review,” *Magazine of Concrete Research*, Vol. 41, No. 147, pp. 51-61, June, 1989.

39. ASTM, “Standard Test Method for measurement of rate of absorption of water by hydraulic cement concretes”, *ASTM International*, C 1585 – 04, 2004.

40. Tasdemir, C., “Combined effects of mineral admixtures and curing conditions on the sorptivity coefficient of concrete”, *Cement and Concrete Research*, Vol. 33, pp. 1637–1642, 2003.

41. Ahmed S. F U. and H. Mihashi, “A review on durability properties of strain hardening fibre reinforced cementitious composites (SHFRCC)”, *Cement & Concrete Composites*, Vol. 29, pp. 365–376, Elsevier, 2007.

42. Landau, A. L., “A System for Inhibiting Steel Corrosion in Concrete”, Proceedings, *Conference on Improving Performance of Concrete in Marine Environments*, Hong Kong, pp. 12.1-12.13, June, 1987.

43. Sanjuan, M. A., C. Andrade and A. Bentur, “Effect of polypropylene fiber reinforced mortars on steel reinforcement corrosion induced by carbonation”, *Materials and Structures*, Vol. 31, pp.343-349, 1359-5997/98 RILEM, June, 1998.

44. Guneyisi E., T. Ozturan and M. Gesoğlu, “A study on reinforcement corrosion and related properties of plain and blended cement concretes under different curing conditions”, *Cement & Concrete Composites*, Vol. 27, pp. 449–461, Elsevier, 2005.

45. Perenchio, W. F., "Corrosion of Reinforcing Steel", *ASTM International*, STP169C-EB, pp.164-172, August, 1994.

46. Bertolini, L. M. Carsana and P. Pedeferri, "Corrosion behaviour of steel in concrete in the presence of stray current", *Corrosion Science*, Vol. 49, pp. 1056-1068, 2007.

47. Pourbaix, M. "Lectures on Electrochemical Corrosion", *Plenum Press*, New York – London, 1973.

48. Austin S.A., R. Lyon and M. G. Ing, "Electrochemical Behavior of Steel-Reinforced Concrete During Accelerated Corrosion Testing", *Corrosion*, Feb. 2004; 60, 2; ProQuest Science Journals, p. 203, February, 2004.

49. Gonzalez, J. A., S. Feliu and P. Rodriguez, "Threshold Steel Corrosion Rates for durability Problems in Reinforced Structures", *Corrosion*; Jan 1997; 53; 1; ProQuest Science Journals, p. 65, January, 1997.

50. Day W. K., "Concrete Mix Design, Quality Control and Specification", Second Edition, *E & FN Spon*, London, 1999.

51. Soylev, T. A. and M. G. Richardson, "Corrosion inhibitors for steel in concrete State-of-the-art report", *Construction and Building Materials*, Vol. 22, pp. 609–622, Elsevier Ltd., 2008.

52. Sağlam A.R., N. Parlak, Ü.A. Doğan and M. H. Özkul, "The Effect of Different Chemical Admixtures on Permeability Properties of Concrete", *Sixth International Congress on Advances in Civil Engineering*, Bogazici University, Istanbul, Turkey, 6-8 October, 2004.

53. Fernàndez-Altable, V. and I. Casanova, "Effect of Superplasticiser Dosage on The Time Evolution of Rheological Behaviour of Cement Pastes at Different Temperatures", *Sixth International Congress on Advances in Civil Engineering*, Bogazici University, Istanbul, Turkey, pp.989-997, 6-8 October, 2004.

54. Jin, X. and Z. Li, "Investigation on mechanical properties of young concrete", *Materials and Structures*, Vol. 33, pp 627-633, 1359-5997/00, RILEM, December, 2000.

55. Detwiler, R. J., K. O. Kjellsen and O. E. Gjorv, "Resistance to Chloride Intrusion of Cured at Different Temperatures", *ACI Materials Journal*, Vol. 88, No.1, January-February, 1991.

56. Tae-Hyun Ha, Srinivasan Muralidharan, Jeong-Hyo Bae, Yoon-Cheol Ha, Hyun-Goo Lee, Kyung-Wha Park and Dae-Kyeong Kim, "Accelerated short-term techniques to evaluate the corrosion performance of steel in fly ash blended concrete", *Building and Environment*, Vol. 42, pp. 78–85, Elsevier, 2007.

57. Caré, S. and A. Raharinaivo, "Influence of impressed current on the initiation of damage in reinforced mortar due to corrosion of embedded steel", *Cement and Concrete Research*, Vol. 37, pp. 1598–1612, Elsevier, 2007.

58. Maaddawy, T. A. E. I. and K. A. Soudki, "Effectiveness of Impressed Current Technique to Simulate Corrosion of Steel Reinforcement in Concrete", *Journal of Materials in Civil Engineering*, Vol. 15, No. 1, February, 2003.

59. Callister W. C. Jr., "Materials Science and Engineering: An Introduction", 5th Edition, *John Wiley & Sons Inc.*, New York, 2000.